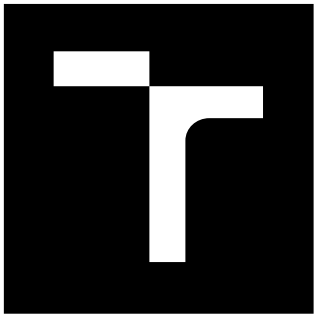

BRNO UNIVERSITY OF TECHNOLOGY
VYSOKÉ UČENÍ TECHNICKÉ V BRNĚ

FACULTY OF MECHANICAL ENGINEERING
FAKULTA STROJNÍHO INŽENÝRSTVÍ

INSTITUTE OF MATERIALS SCIENCE AND ENGINEERING
ÚSTAV MATERIÁLOVÝCH VĚD A INŽENÝRSTVÍ

INFLUENCE OF LAMINE THICKNESS ON BIFURCATION APPEARANCE IN CERAMIC LAMINATE
VLIV TLOUŠŤKY VRSTEV KERAMICKÉHO LAMINÁTU NA BIFURKACI TRHLINY

MASTER'S THESIS
DIPLOMOVÁ PRÁCE

AUTHOR — **Bc. Kristina Sorokina**
AUTOR PRÁCE

SUPERVISOR — **Ing. Hynek Hadraba, Ph.D.**
VEDOUCÍ PRÁCE

BRNO 2016

BRNO UNIVERSITY OF TECHNOLOGY
FACULTY OF MECHANICAL ENGINEERING

Specification Master's Thesis

Department:	Institute of Materials Science and Engineering
Student:	**Bc. Kristina Sorokina**
Study programme:	Applied Sciences in Engineering
Study branch:	Materials Engineering
Leader:	**Ing. Hynek Hadraba, Ph.D.**
Academic year:	2015/16

Pursuant to Act no. 111/1998 concerning universities and the BUT study and examination rules, you have been assigned the following topic by the institute director Master's Thesis:

Influence of lamine thickness on bifurcation appearance in ceramic laminate

Concise characteristic of the task:

Ceramic layered materials (laminates) combine different materials to achieve change in the physical properties of the composite, and therefore in its behavior. One approach is to prepare a laminate of two alternating materials so that the layers of the laminate contain residual stresses. During fracture of the ceramic laminate the bifurcation of the cracks can be observed. This process consumes a considerable portion of energy and is therefore responsible for a significant increase in crack resistance of the ceramic laminate. If the size of the internal residual stresses is sufficiently large, the edge cracks parallel to the interface layers can be developed. The edge cracks development can be connected to the crack bifurcation. This work will be focused on proving of this assumption.

Goals Master's Thesis:

The aim of the work is to find and experimentally verify relationship between critical thickness of the layers controlling the formation of edge cracks in the ceramic laminate and bifurcation of the crack, or find a way how to affect the cohesion of the interface layer in the laminate to control the behaviour of cracks at the interface between two layers. The students will prepare of multilayer ceramic materials using electrophoretic deposition and suspension casting, preparation of samples for testing of the mechanical properties and perform mechanical tests and theirs evaluation.

List of literature:

Hadraba, H., Klimeš, J., Maca, K.: Crack propagation in layered Al2O3/ZrO2 composites prepared by electrophoretic deposition. Journal of Materials Scince 42 (2007) 6404-6411.

Hadraba, H., Drdlik, D., Chlup, Z., Maca, K., Dlouhy, I., Cihlar, J.: Laminated alumina/zirconia ceramic composites prepared by electrophoretic deposition. Journal of the European Ceramic Society 32 (2012) 2053–2056.

Chlup, Z., Hadraba, H., Slabakova, L., Drdlík, D., Dlouhy, I.: Fracture behaviour of alumina and zirconia thin layered laminate. Journal of the European Ceramic Society 32 (2012) 2057–2061.

Deadline for submission Master's Thesis is given by the Schedule of the Academic year 2015/16

In Brno,

L. S.

prof. Ing. Ivo Dlouhý, CSc.
Director of the Institute

doc. Ing. Jaroslav Katolický, Ph.D.
FME dean

ABSTRACT

In layered ceramic composite materials the internal residual stresses occur due to thermal expansion coefficient mismatch of individual layers. During cooling of layered composite from sintering temperature the layers start to shrink with different rate according to the thermal expansion coefficient. Permanent compressive and tensile residual stresses generate in individual layers if they are strongly bonded together. Magnitude of the residual stresses is controlled by volume ratio between two combined materials. In this work, ceramic laminates consisted of 7 and 9 alternated layers combining two different ceramic materials were prepared by sequential slip casting and electrophoretic deposition and subsequently studied. The prepared laminates were analyzed for existence of edge cracks in layers containing compressive residual stresses. By using results of 2D parametric numerical model and combination of compressive residual stress and layer thickness, the prediction of presence and absence of edge cracking were compared with the actual presence and absence of edge cracks in compressive layers. The crack bifurcation caused by edge cracks presence was studied on the 3D fracture surfaces reconstruction of laminate prepared after testing of flexural strength.

KEYWORDS:
ceramic laminates, electrophoretic deposition, suspension casting, mechanical testing.

ABSTRAKT

Z důvodu rozdílných koeficientů délkové teplotní roztažnosti jednotlivých vrstev vzniká ve vrstvách keramického vrstevnatého kompozitního materiálů reziduální napětí. V průběhu chladnutí vrstevnatého kompozitu ze slinovací teploty jednotlivé vrstvy smršťují různými rychlostmi v závislosti na velikosti koeficientu délkové teplotní roztažnosti. Jestliže jsou tyto vrstvy spolu pevně spojeny vzniká v jednotlivých vrstvách různě velké trvalé zbytkové napětí. Velikost residuálního napětí je dána objemovým podílem obou složek v kompozitu. Tato práce byla zaměřena na přípravu a popis 7-mi a 9-ti vrstevných keramických laminátů složených ze střídajících se vrstev dvou rozdílných materiálů. Keramické lamináty byly připraveny pomocí metody suspenzního lití a elektroforetické depozice. U připravených laminátu byl sledován vznik tzv. hranových trhlin (edge cracks) ve vrstvách obsahujících tlaková zbytková pnutí. Výsledky pozorování přítomnosti hranových trhlin pro různou konfiguraci velikosti zbytkových napětí a tloušťky vrstev byly srovnány s teoretickou předpovědí vytvořenou pomocí parametrického 2D

modelu. Vliv vzniklých hranových trhlin na průběh lomu byl studován pomocí 3D rekonstrukce lomového povrchu po ohybové zkoušce připravených vrstevnatých kompozitů.

KLIČOVA SLOVA

keramické lamináty, elektroforetická depozice, suspenzní lití, mechanické zkoušky.

BIBLIOGRAPHIC CITATION

SOROKINA, K. *Influence of lamine thickness on bifurcation appearance in ceramic laminate*. Brno: Brno University of Technology, Faculty of Mechanical Engineering, 2016. 73 p. Supervisor of master's thesis Ing. Hynek Hadraba, Ph.D..

DECLARATION

I, Bc. Kristina Sorokina, declare that I have developed the submitted master's thesis independentlyand that I stated all used sources and literature.

Brno, _____

Kristina Sorokina

ACKNOWLEDGMENT

At this point I would like to thank my supervisor Ing. Hynek Hadraba, Ph.D., who helped me greatly in addressing this work. Also thank all the staff of the Group of brittle fracture IPM ASCR for their friendly approach. Finally, thank also to the Department of ceramics and polymers at FME.

CONTENTS

1 INTRODUCTION

Research in the field of advanced materials and technologies is focused not only on efficiency and usability of the product, but also on its affordability. Among materials satisfying these conditions, ceramic materials can be identified. Ceramic materials are inorganic non-metallic materials, containing metallic or non-metallic elements, associating with ionic, covalent and sometimes metallic bonding. The chemical composition of ceramic materials ranges from the simplest compounds to the mixtures of complicated phases [1]. Ceramic materials have attractive properties such as high hardness, high melting point, excellent chemical resistance and low density. On the other hand, these materials suffer from certain limits in case of deformation. They are very sensitive to stress concentrators (holes or cracks) and contact stress due to absence of formability.

Besides traditionally used advanced ceramics, there are also ceramic composite, which are widely used. In certain applications composite ceramics replace the existing materials for reason of improved properties. For example, it can replace monolithic ceramics in terms of the negative values of mechanical properties, especially brittleness. Composite ceramic is strengthened by particles, fibers, whiskers or creation of layered ceramics [2], which is one of the goals of this work.

The research in the field of materials is aimed to achieve quite specific material properties. The trend can be connected to so-called tailored materials or functionally gradient materials. The concept of functionally gradient material relates to a heterogeneous material whose structural components are deliberately unevenly distributed. The result of changes in the composition is the changes of chemical and physical properties in certain directions. The basic example of the functional gradation of material properties is the interface of two materials with different physical properties.

Layered materials are used in industry for a long time. The engineering laminates that consist of layers of ceramic materials are used in specialized applications [3]-[6]. Layered materials have fracture mechanical properties better than the original materials of individual components. The presence of interface and related thereto intermittent changes of material properties leads to redistribution of stresses in the body and by this to influence to crack behaviour. It can be stated, that in some cases the existence of interface in the composite can function as barrier against crack propagation, and sometimes can function as place of crack initiation [7].

There are two basic types of layered ceramics on the literature: composites with weakly bonded layers [8] and composites with strongly bonded layers [9]. The physical mechanisms of

the stress transfer through the layer interface in these two types of composite are different, and also the mechanisms of crack propagation across the layer interface are different. In the composites with weakly bonded layers the deflection of a crack propagation in the interface of two materials, which leads to an increase of fracture toughness of the composite, can be observed. This mechanism leads to an increase of fracture toughness of composites accompanied with decrease in strength, that prevents use them in structural applications. In composites with strongly bonded layers, in contrast, the deflection (or bifurcation) of crack propagation can be observed when the crack extends through the interface of two materials. This mechanism also allows to increase the fracture toughness, but without decrease in the other mechanical properties. Moreover, it can be used at such temperatures that in certain cases it does not effect to the transformational strengthening of ceramics. The observed deflection and bifurcation are usually explained by the existence of residual stresses near the interface of two phases.

The aim of this work is preparing the ceramic laminates based on Al_2O_3 and ZrO_2 (both tetragonal and monoclinic ZrO_2 phase) containing tensile and compressive residual stresses. The development of edge cracks inside the laminates will be studied as a consequence of residual stresses distribution. The appearance of edge cracking inside the ceramic laminates will linked to final crack behaviour during flexural tests and to final strength of the laminates.

2 THEORETICAL PART

2.1 General theory of ceramic laminates

2.1.1 Causes of high brittleness of ceramics

The characteristic feature is connected to the ceramic material – the brittleness. Brittleness of any material is caused by limited ability of plastic deformation. There are several causes of limited plasticity of the ceramic materials that lie in physical and/or chemical nature of the ceramics.

The first reason for limited plasticity of ceramic materials is caused by type of chemical bonds (ionic and covalent) between atoms. Strength of the chemical bonds is comparable to the bond strength of metal, but differs in the distribution of electric charges and a distinctive directionality. The atomic bonds have a direct influence to mobility of dislocations in a material, through which the process of plastic deformation of the material is going [1]. Required stress for the movement of dislocations (Peierls-Nabarro stress, below PN stress) is in magnitude of several GPa in the case of ceramics. Therefore stress value should be close to the ideal value of the strength of the material for the plastic deformation of ceramics. Besides the strong covalent crystals, some ionic crystals with complex lattice and a big value of Burgers vector ($MgO \cdot Al_2O_3$) have high values of PN stress. In these cases, formability is already limited in single crystals due to the low mobility of dislocations.

The second reason for limited plasticity of ceramic materials lies in low plasticity of ionic ceramics with simple crystal lattice (MgO, ZrO_2). Values of the PN stress in this type of materials are relatively low and their monocrystals are quite easily able to plastic deformation. In the case of the polycrystalline material a considerable limitation of the number of geometric planes and directions of strength occurs, that is leading to failure Mises yield criterion plastic deformation of the polycrystalline material (five independent of slip systems are necessary in the case of plastic deformation of the polycrystalline material). A low maneuverability of dislocations can be identified as the reason for difficulty of the plastic deformation of the polycrystalline ceramic material.

The third cause of low formability of ceramics is the combination of both above-mentioned properties - low mobility and maneuverability of dislocations. Materials such as Al_2O_3 and SiO_2 belong to this group.

There are several possibilities for increasing of the toughness of ceramics identified by the author of work [1]. One of them is targeted changes in the chemical composition of the material to affect mentioned mobility or maneuverability of dislocations. The effort to reduce the so-called transition temperature is also associated with this approach. With increasing

temperature the thermal activation facilitates the migration of dislocations through the PN barriers. The PN stress decreases and dislocation motion along the slip side systems is also possible; the number of the slip system increases and thus the maneuverability of dislocations is improving. The thermal activation ultimately enhances the formability of ceramics. This temperature is very high, reaching approximately eight-tenths of the melting point.

Other possibilities arise from the technology of production of ceramics. There are several approaches based on using of nanocrystalline materials (reduction of size of natural flaws, higher absorption of energy by fracture branching in processing zone in crack tip front) and on using of materials with high grain boundary strength of and low content of structural defects (e.g. pores). The most traditional way of ceramics toughening is based on utilization of phase transformation. Most significant example of this approach is the utilization of tetragonal ZrO_2, which undergo phase transformation during loading accompanied with volume change contributing to energy absorbing during the crack propagation. Finally, the development of multiphase ceramic systems and ceramic composites can not be overlooked.

2.1.2 Strengthening mechanisms

Polycrystalline ceramics contain many different sized defects. When ceramic is loaded by stress that is less than a critical, it occurs to the plastic deposition of energy within the material. Upon reaching the critical stress crack begins to initiate at the largest appropriately oriented defect and the accumulated energy is concentrated at the crack tip. Conventional ceramics cannot effectively prevent it and crack propagates so quickly through the material, leading to a sudden brittle failure. The aim is to produce a tough ceramic that is resistant to the energy concentration at the crack tip, or that can dissipate this stored energy. Dissipation of energy can be achieved by utilization of one of the toughening mechanisms [10].

2.1.2.1 Strengthening of monolithic ceramics

Transferring of elastic modulus

Applied stress to the composite is "transferred" from the matrix to the fibres so that the strong fibres carry the tensile load. The fibres should have modulus of elasticity at least 2 times larger than the surrounding matrix. Unidirectional laid fibres (1D) provide toughening and strengthening only in a perpendicular direction to the fibres. The fibres can be continuous or short. In order to transfer the stress from the matrix to the fibres, the bond between the fibres and the matrix must be sufficiently strong [10].

Pre-stress

Fracture of ceramic materials usually occurs in tension, which leads to the opening of the crack. From this perspective, appears as appropriate concept to expose part of ceramics to the residual compressive stress, i.e. to pre-stress it. If ceramic is pressure-preloaded, the crack can not originate and/or to extent. Fracture arises only if the applied stress is high enough to overcome the preload of the pressure and to create a sufficiently large tensile stress at critical size defect.

The preload arises due to rapid cooling of the surface, ion exchanges or layering. Further, in the fibre composite wherein the fibres are pre-stressed during manufacturing in order for subsequent compression of the matrix after unloading. Fibres must be strong enough and there must be a strong bond between the fibres and the matrix. An example is a concrete with metal bars [10].

A more frequent example is preloaded surface. It can be achieved by heating the material close to a melting temperature with subsequent rapid cooling of surface. Since the material is still warm inside the compressive stress arises on the surface during cooling. The safety glass can be as an example of this approach.

The residual stress can originate due to the difference of thermal expansion of fibres and matrix. The matrix is formed around the fibres at elevated temperature. After cooling, the higher thermal expansion of fibres results caused their greater shrinkage compared to the matrix in which they form a compressive stress. The different coefficient of thermal expansion is also important in multilayer materials where the aim is to obtain the pressure field on the surface [10].

Diversion of crack

Fracture toughness is closely related to the microstructure of the ceramic. If crack propagates directly and the newly formed surface is minimal, little energy was consumed. Such fracture can occur in glasses or single crystals - fracture surface is smooth, with no visible barriers. These materials exhibit low fracture toughness [10].

In polycrystals each grain is differently oriented, and therefore crack can not spread straight but deflects to the barriers. Therefore, newly formed surface covers a larger area than in single crystals. Fracture toughness increases more than twofold. From the above mentioned it follows that the toughness can be increased by appropriate modification of the microstructure, e.g. by grain size extent, dispersion of secondary particles, whiskers, short fibres or adding an additional phase. The increase in toughness depends on the volume and shape of the particles (spherical particles - about twice, fibres up to four fold increase) [10].

Crack bridging

The bridging that prevents the crack opening is the main toughening mechanism in composites with long fibers (see Fig. 2.1). During the loading, the crack starts to propagate through the matrix, but fibres near the crack tip have sufficient rigidity and strength in order to be not violated, also it leads to reduction in the stress concentration at the crack tip and slows or stops its propagation. For extension, pulling out or breaking of fibres the additional energy must be supplied. After overcoming this energy the crack can spread further. This mechanism applies not just for fibre composites, but also for ceramic reinforced by particles or whiskers. The crack bridging occurs also if the plastic phase extends, that thereby is preventing crack opening [10].

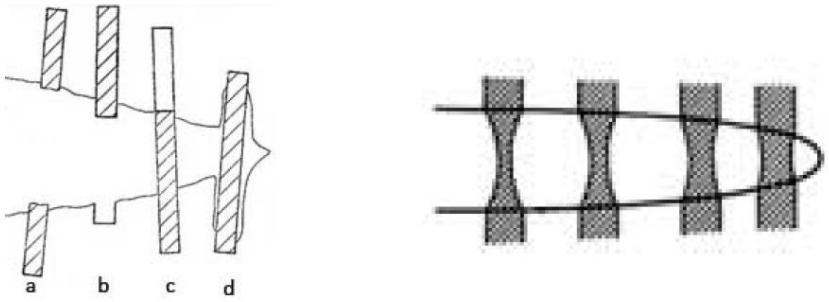

Fig. 2.1. Examples for crack bridging by short fibres [28] (1, a- fracture fibre, b- crack bypassing the fibre, c - pull-out, d - tearing, 2, bridging by plastic fibres)

Pull-out

Pull-out means extension of the fibres, particles or grains from the surrounding matrix during the opening cracks. Energy, which sometimes leads to crack propagation, is partly consumed for breaking the bonding and friction between fibres (particles, grains) and the surrounding microstructure (matrix). This causes an increase in fracture toughness. As well as the bridging, which often accompanies, it is most often observed in fibres composites. The main characteristic is the nature of the interface fibre/matrix, which must not be too strong to avoid breaking of fibres in the trajectory of cracks before pulling out [10].

2.1.2.2 Strengthening by composites manufacturing

The other way to improve the mechanical properties of ceramics - manufacture of layered materials - enables to adapt the microstructure and mechanical properties of the material for specific application. Because layered composites are the object of this work, some examples demonstrating the importance and possibilities of this type of material will be shown.

The first example is a layered composite designed to exhibit a high strength in large range of crack lengths. The basis is the production of three-layer composite comprising two outer layers of solid material and an inner layer of a material with a high resistance to crack

propagation [11]. The thickness of the outer layers is chosen so as to obtain sufficient strength of the composite and to maintain the resistance to propagation of a priori cracks (see Fig. 2.2).

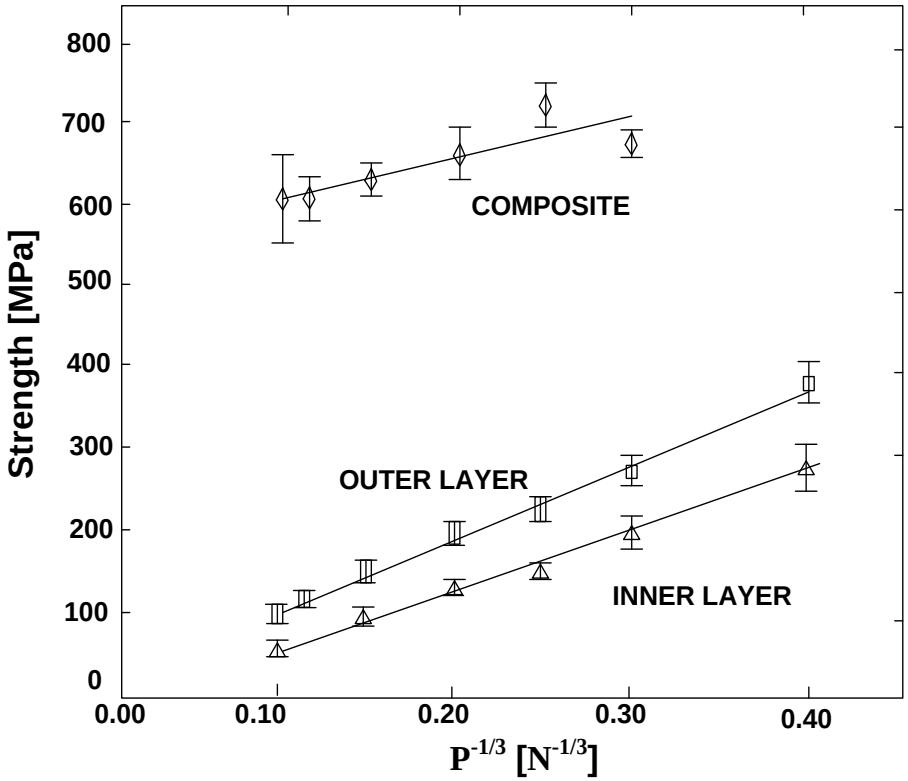

Fig. 2.2. Dependence of strength on the reciprocal value of cube root of indentation load [12].

The second case which will show the advantages of layered composite laminates is the creation of toughening ceramics (tetragonal ZrO_2), which reach by themselves the fracture toughness from 10 to 20 MPa*$m^{1/2}$. Transformation zone in these materials have incline to extend very far ahead of the crack in some cases, until a distance of 20 times greater than the width of the transformation zone, leading to a decrease in fracture toughness. It is assumed that this decrease is caused by the presence of monoclinic ZrO_2, which has low fracture toughness. Large quantities of a priory cracks also affect reducing of the fracture toughness in front of the main crack, as a result of volume changes in the transformation of tetragonal ZrO_2 to monoclinic ZrO_2. Marshall [13] determined that the fracture toughness can be doubled by limiting the length of the transformation zone on dimensions comparable to the width of the zone. To prevent overtaking the phase transformation layered materials with a thickness of 10-100 μm were used, which represented a barrier to excessive expansion of the transformation zone. Simultaneously expansion of transformation occurred along the interface, that was perpendicular to the direction of crack propagation, which further increased the fracture toughness that ranged from 20 to 48 MPa*m1/2 (see Fig. 2.3).

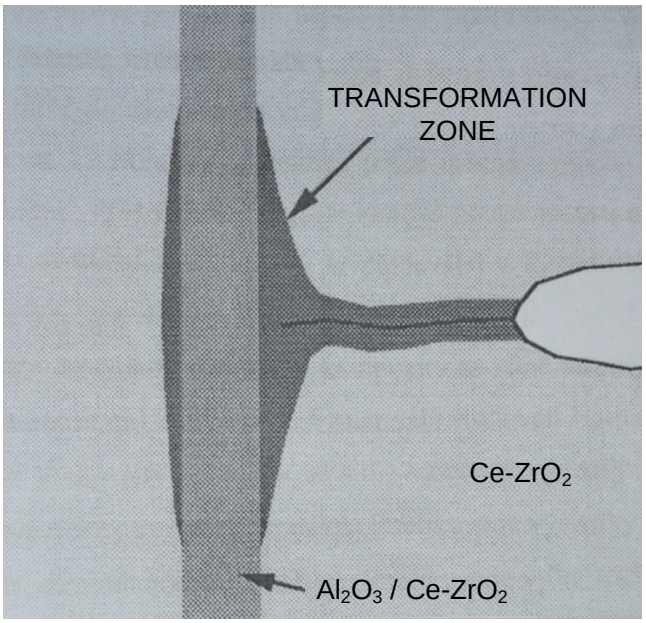

Fig. 2.3. Limitation the length of the transformation zone in tetragonal ZrO_2 by creating the barriers in front of crack tip [14].

2.1.3 Ceramic laminates

Ceramic laminates are composed of layers of different chemical composition and microstructure. The greatest advantage of composite structures, where the ceramic laminates belong to also, is the fact that as a whole they have better characteristics than the monoliths of materials of which they are formed. Nowadays their usability and demand for them is growing due to industry requirements. Production of layered structures is the easiest and cheapest way to effectively combine different materials.

Composite materials of laminar type are used in nature since time immemorial. One example of a layered structure can be shell of sea abalone [15] (Fig. 2.4).

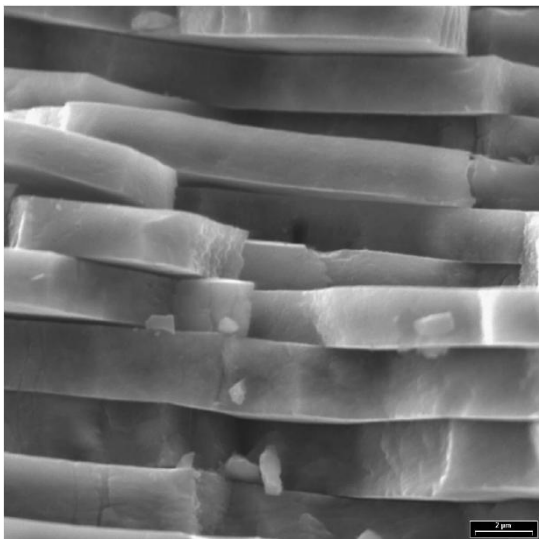

Fig. 2.4. Microphotography of shell of sea abalone [16].

The shell of the shellfish consists of solid nanostructural blocks of calcium carbonate which are combined by organic phases (elastic slime). It is difficult for cracks initiated on the shell surface to penetrate inside the shell. Structure of the shell impedes propagation of the crack, whose pathway is tortuous in overcoming blocks, that leads to dissipation of energy needed to fracture [16].

Type of interfaces between the layers determines the behaviour of the layered material. There are two basic types of interfaces, strong and weak. Ceramic laminates can have low ultimate strength and/or toughness or nearly reach the theoretical strength with excellent adhesion. In the first case is achieved not brittle failure due to significant deviation of the crack; in the second case there is an increase of toughness due to residual stresses.

Laminates with weakly bonded layers

Shell of shellfish that is mentioned above could be categorized as a layered composite with weakly bonded layers. This type of lamellar structure is a cheap and easy way to tough ceramic [8].

Weak interfaces between the layers can be achieved in several ways. The first way is addition a suitable material between layers before sintering or formation of a porous interface [17]. Frequently, the examined representative of the first subgroup is a composite of layers of silicon carbide coated with graphite, which creates a thin layer between layers of carbide after sintering [18]. Theoretically, in such material residual stresses could not create despite the different coefficient of thermal expansion. As shown in the second subgroup, the layers may be of different materials. Weak interface can be achieved also by changing the variously porous layers of the same composition. Due to the uniform composition the residual stresses do not arise (porous layer shrinks as the surrounding dense matrix) [17].

Contribution of weak interfaces applies particularly in those laminates in which the crack propagates perpendicularly to the interface. The growing crack turns into a thin layer, which causes delamination between two adjacent thick ceramic layers.

Fig. 2.5 shows the force - deflection curve obtained during bending test of specimens with V notch. Two materials of the same composition were investigated, one monolithic and the second with weakly bonded layers. In the first part of graph, both materials behave identically under load. In the area indicated by an asterisk monolith and the first layer laminate break. With the rising forces crack veers to the interface, where the delamination occurs. Slope of the curve is smaller due to a smaller remaining cross-section. The new crack initiation occurs in the next layer; layer cracks and fracture diverts to the interface again at reaching of maximum of fracture

stress. Fracture continues by this mechanism. The force-deflection curve has a saw-tooth shape that is typical for the stepped fracture of laminates with a weak interface [17].

As mentioned in the example, the crack does not initiate after delamination at the crack tip, but at the defect within a layer, usually near the centre where the high stress is. The strength of this type of laminate is so determined strength of individual ceramic layers. Toughness of laminates can grow up to 4 times compared to monoliths, impact strength even more than 100 times [17].

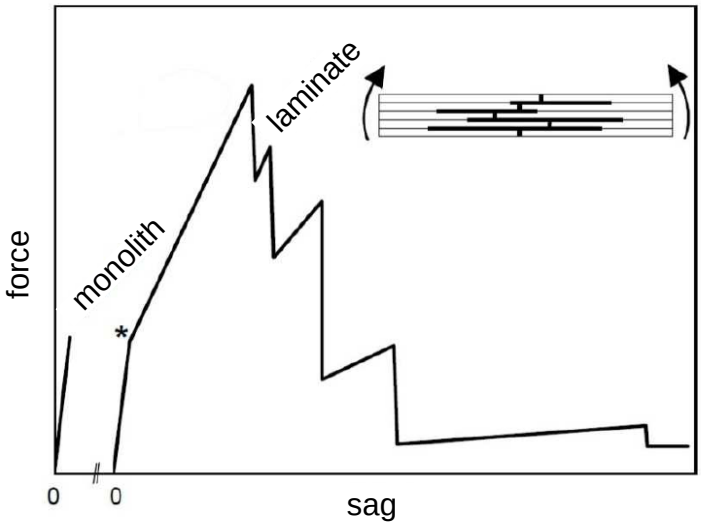

Fig. 2.5. Course of loading of the monolith and laminate is weakly bonded layers, and drawing of laminate after testing [17].

Clegg et al. [8] presented similar results; they examined the laminate composed of layers of SiC/C in proportion 19:1. Fracture toughness of laminate increased 4 times (from 3.6 MPa*$m^{½}$ (SiC) to 15 MPa*$m^{½}$ (laminate)).

Simultaneously with the increase of fracture toughness, unfortunately, the strength and cohesion of the material decrease. Hence, this type of ceramic is not suitable for all applications [19].

In laminates with layer structure there is delamination in two directions that leads to loss of integrity. This fact prevents to massive expansion. Solutions can be found in the nature and structure of the board can be replaced by concentric cylindrical as for example in strain of the tree. The change of board structure into self-sealing ring leads to reduction of direction of delimitation from two until none.

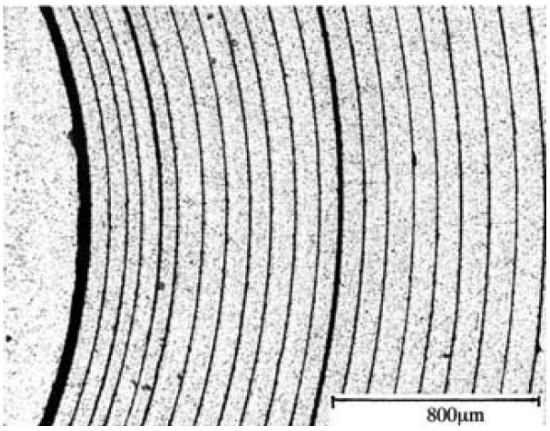

Fig. 2.6. Photo of laminate SiC/C - gray are high density layers of SiC, black are porous layers of SiC (formed from graphite) [18].

Compared to the monolith and the board laminate the main advantage of the ring structure is that the during crack propagation the material is holding together. In comparison with SiC monolith, strength decreased only about one and half times, while the fracture toughness increased for 2-4 times, but mainly the sudden failure did not occur [18].

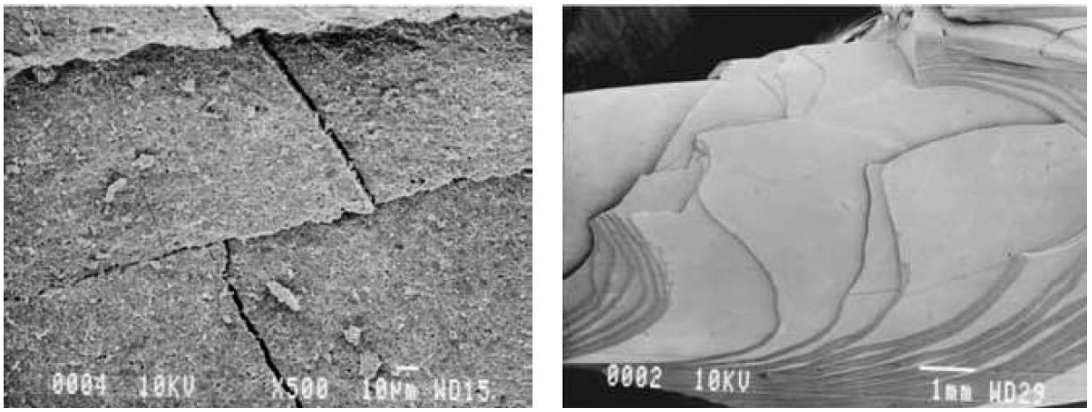

Fig. 2.7. The fracture surface of SiC/C (30:1), diverted crack between layers [18].

Fig. 2.7 shows that body holds together despite the progressive delamination. The gradual fracture is similar to composites that are reinforced by unidirectional oriented continual fibres. Production of laminate is significantly easier and cheaper.

Laminates with strongly bonded layers

The second group includes layered composites with strongly bonded layers. This group shows a sharp change in mechanical and physical properties at the interface, which is usually very thin [20]. Compared to above mentioned laminates with weakly bonded interface the laminates with strongly bonded interface have an enormous advantage that their strength characteristics do not decrease [15], [19]. The development of layered structures with strongly bonded interface was based on the assumption that it is possible to design a material that contains residual stresses. Those residual stresses increase mechanical and tribological properties of the material [11].

Residual stresses arise in the layered material due to differences in the technological and physical behaviour of individual components.

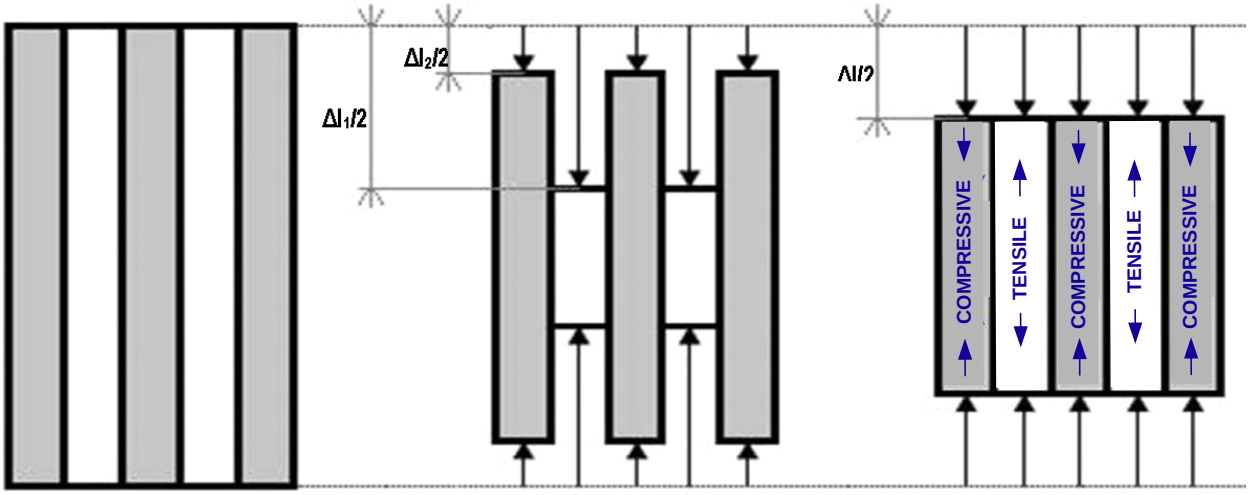

Fig. 2.8. Creation of thermal residual stresses (a, sintering temperature, without tension, b, shrinkage of unbonded layers during cooling; c, creation of residual stress due to cooling of strongly bonded layers).

Relatively high levels of residual stress can be achieved in materials with strongly bonded layers due to a difference in thermal expansion coefficient and elastic modulus [15], [11], [19], [21]. Specifically, residual stresses are created during cooling from the sintering temperature (see Fig. 2.8).

Formation of cracks in the layers containing tensile stress, deformation of the shape and delamination [22] may be a risk of toughness mechanism, so it is very important to control accurately both the size and distribution of residual stress [11].

Materials with residual stresses exhibit a higher strength, toughness, and better resistance to abrasion than monolithic materials (which the laminate is composed of). The composite that is based on alumina and zirconia belongs to the most studied ceramic materials with strongly bonded layers. This is for several reasons. It has excellent bonding of layers without excessive diffusion between components, also has good thermo-mechanical properties and it is relatively easily manufactured. The difference in coefficient of thermal expansion between aluminum and zirconium oxide is 1×106, which is sufficient to create a strong field of residual stress that is needed for improving the mechanical properties, but still does not affecting the reliability of the whole structure [11].

Value of the tensile stress in the layer of zirconium oxide can be described the following equation (2.1) [19]:

$$\sigma_{rAl_2O_3} = \frac{\left(\alpha_{ZrO_2} - \alpha_{Al_2O_3}\right) * \Delta T * E_{ZrO_2}}{1 - \nu_{ZrO_2}} * \left(1 + \frac{\overline{t_{ZrO_2}}}{\overline{t_{Al_2O_3}}} * \frac{\frac{E_{ZrO_2}}{1 - \nu_{ZrO_2}}}{\frac{E_{Al_2O_3}}{1 - \nu_{Al_2O_3}}}\right)^{-1} \quad (2.1)$$

where $\overline{t_{ZrO_2}}$ and $\overline{t_{Al_2O_3}}$ $[\mu m]$ is the average layer thickness, ν_{ZrO_2}, $\nu_{Al_2O_3}$ [-] is Poisson's ratio, α_{ZrO_2}, $\alpha_{Al_2O_3}$ [K^{-1}] is the coefficient of linear thermal expansion and E_{ZrO_2}, $E_{Al_2O_3}$ [MPa] is the elastic modulus of the zirconia and alumina, respectively.

Note: the compressive stress in the Al_2O_3 layer is obtained by changing indexes, i.e.:

$$\sigma_{rAl_2O_3} = \frac{\left(\alpha_{Al_2O_3} - \alpha_{ZrO_2}\right) * \Delta T * E_{Al_2O_3}}{1 - \nu_{Al_2O_3}} * \left(1 + \frac{\overline{t_{Al_2O_3}}}{\overline{t_{ZrO_2}}} * \frac{\frac{E_{Al_2O_3}}{1 - \nu_{Al_2O_3}}}{\frac{E_{ZrO_2}}{1 - \nu_{ZrO_2}}}\right)^{-1} \quad (2.2)$$

From the above mentioned equations, it is clear that the residual stresses depend on the ratio of the thicknesses of the individual layers, so composite with different high tension in the layers can be produced by their simply changing.

At the interface between two materials residual stress leads to a change in the direction of spreading cracks that is resulting to increase in fracture toughness while maintaining a high strength and other mechanical properties [15]. It is known that the a priori crack that is oriented perpendicularly to the direction of tensile stress spreads perpendicularly to it (see Fig. 2.9a). The crack is trying to curl perpendicular to this stress by applying tension stress to plane of crack. Conversely, crack that is parallel to the direction for compressive stress spreads parallel to it (see Fig. 2.9b).

From this concept, mechanism of crack propagation in the layered material is based. As shown in Fig. 2.9, the direction of action of residual stresses is parallel with layers. The crack in the layer with compressive stress turns toward the interface, and conversely away from the interface layer which contains the tensile stresses.

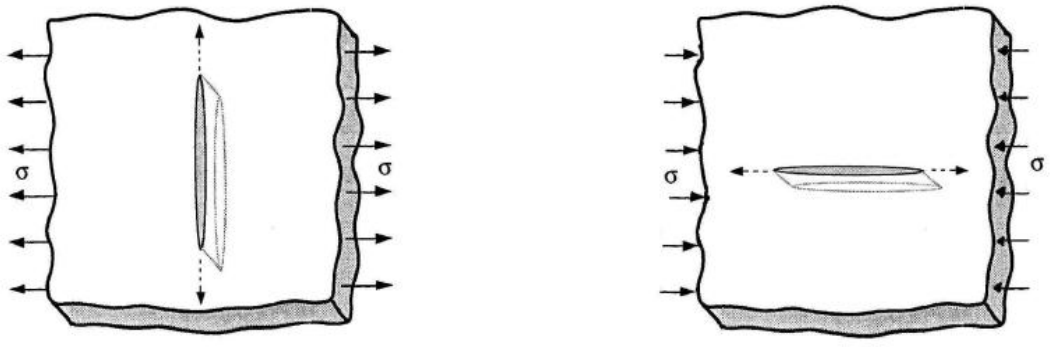

a) **b)**

Fig. 2.9. The spread of cracks in tension (a) and compressive (b) field.

The explanation will be given in a specific example for understanding. As seen from the macrophotography in Fig. 2.10, crack in the tensile stress field of ZrO2 deviates from the interface of layers ("opens"). During the passing through the interface to the layer of Al_2O_3, conversely, crack turns to the interface in order to approach to the parallel direction with the compressive stress in this layer.

From Fig. 2.10 is seen that the direction of crack propagation is repeated and it is parallel in individual layers of the same material - see $\Delta\alpha_{ZA} = \Delta\alpha_{AZ}$ in Fig. 2.10.

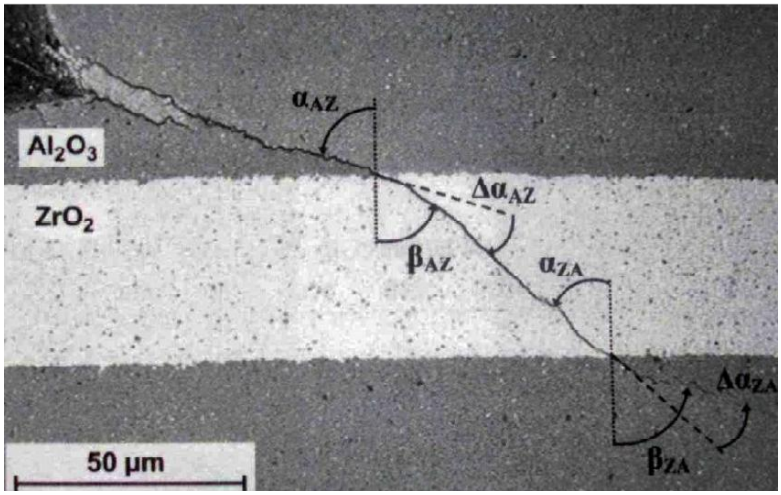

Fig. 2.10. Propagation of cracks in the composite Al_2O_3/ZrO_2 [22].

Crack propagation that is initiated from the imprint was examined depending on the different inlet angles. It was found that in a perpendicular direction to the interface, there is no deflection in the direction of crack propagation. Conversely, if the crack propagates at an angle of 45°, the greatest deflection occurs at the interface, which in this case was 15° [22].

Samples with different ratios of layer thicknesses, and with significantly different values of residual stresses, exhibited approximately the same deflection of cracks during the indentation. Therefore, it could be suggested that the deflection of crack does not occur due to residual stresses, but it occurs due to changes in elastic modulus between the layers and due to the presence of strongly bonded interface [22]. This hypothesis was confirmed only near to the surface, which the stress effects. In the inner layers bigger deflection of cracks was observed due to residual stresses.

Hatton and Nicholson [21] studied behaviour of layered ceramics based on Al_2O_3/ZrO_2 at different temperatures. It was found that with increasing temperature fracture behaviour changes from spontaneous delamination over the fracture behaviour with deflection of crack to sudden fractures with and without deflection of cracks (see Fig. 2.11). This example could be evidence of the effects of residual stresses on crack propagation. With increasing temperature the material returns to the conditions during sintering, when no stress was in material.

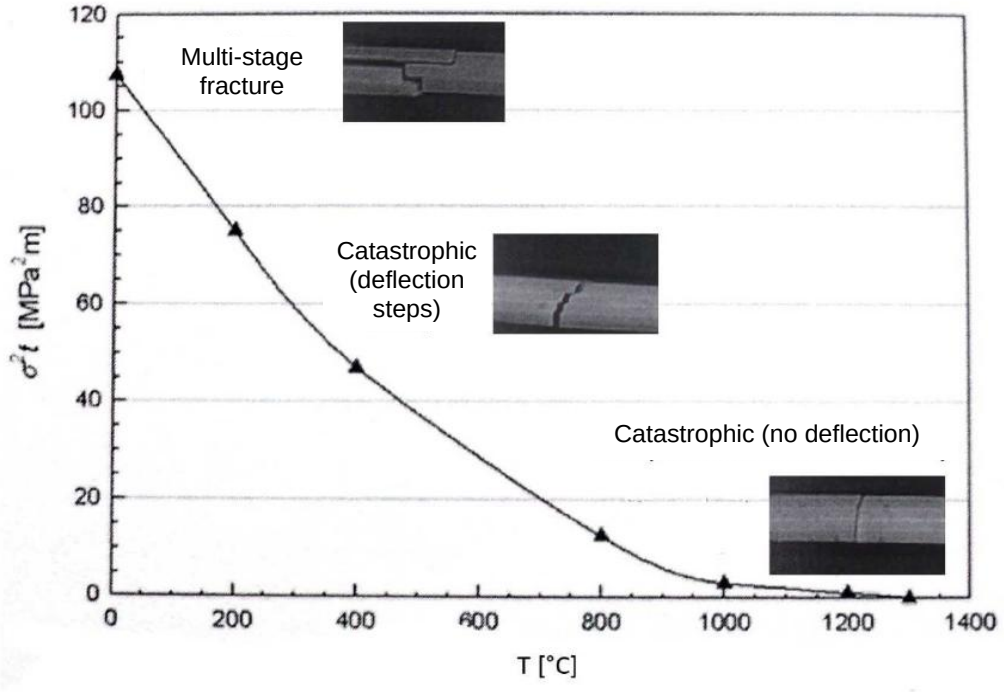

Fig. 2.11. Crack propagation depending on temperature [19], [21].

In addition to above mentioned ceramic laminates with strongly bonded layers there are multilayered ceramics that contain Al_2O_3 + $tZrO_2$ (ATZ) and Al_2O_3 + $mZrO_2$ (AMZ) layers. These layers were designed to explore the effect of spatially-dependent residual stress and layer distribution on mechanical behaviour [23].

In work of Chang Y. et al. [23] composites of Al_2O_3 + 5 vol.% $tZrO_2$ (ATZ) and Al_2O_3 + 30 vol.% $mZrO_2$ (AMZ) layers were used. The addition of 5 vol % tetragonal zirconia in ATZ has the effect of limiting alumina grain growth during sintering. The 30 vol. % of monolithic zirconia was used in the AMZ layer to generate a large strain mismatch between the AMZ and ATZ layers. When they were cooled from the sintering temperature, some of the zirconia in the layers transformed to the monoclinic form. This was a result of the ~5% volume change during the t→m transformation ~730℃ and those induce a high residual compressive stress when embedded in the ATZ matrix [24], [25].

In particular, these multilayer composites designed with strong interfaces can present enhanced mechanical behaviour through microstructural design and due to the presence of compressive residual stresses arisen due to different coefficients of thermal expansion, acting as a barrier to crack propagation.

For a multilayer system composed of n layers of composition A and thickness t_a and $(n-1)$ layers of composition B and thickness t_b, the residual stress within each layer can be calculated by equations (2.3) and (2.4) [24]:

$$\sigma_a = -\frac{\Delta\varepsilon E'_a}{1 + \frac{E'_a n t_a}{E'_b (n-1) t_b}} \tag{2.3}$$

$$\sigma_b = \frac{\Delta\varepsilon E'_b}{1 + \frac{E'_b (n-1) t_b}{E'_a n t_a}} \tag{2.4}$$

where $E'_i = E_i/(1-\nu_i)$, being E_i the Young's modulus and ν_i the Poisson ratio of a given layer. The stress in one layer is related to the stress in the adjacent one by (2.5)

$$\sigma_b = -\sigma_a \frac{n t_a}{(n-1) t_b} \tag{2.5}$$

From these basic formulas Bermejo in his work [15] extracted some qualitative analysis taking into account the number and thickness of the layers: "First, if $n \gg 1$and $t_a = t_b$, then $\sigma_a = -\sigma_b$, i.e. for a laminated system with a high number of layers of the same thickness, the tension of an inner layer is equal to the compression of the adjacent one. Second, if $t_a \ll t_b$ then $\sigma_a \to 0$, i.e. if thin layers are inserted between thick ones, the stresses inside the latter are negligible. This allows the fabrication of laminar ceramics with high internal compressive stresses at thin layers combined with thick layers exhibiting tensile residual stresses whose effect on the final strength of the material is not significant".

In case of layered structures, the difference in coefficients of thermal expansion between the corresponding layers may induce macrostresses in the sintering step, since they are subjected to temperature changes from the sintering to room temperature. In this investigation in work [15], the differential dilatometer was used for estimating the coefficient of thermal expansion of the ATZ and AMZ of the laminates that was performed through dilatometric tests on sintered ATZ and AMZ specimens. Fig. 2.12 and Fig. 2.13 show the thermal strain evolution of monolithic samples of ATZ and AMZ, respectively.

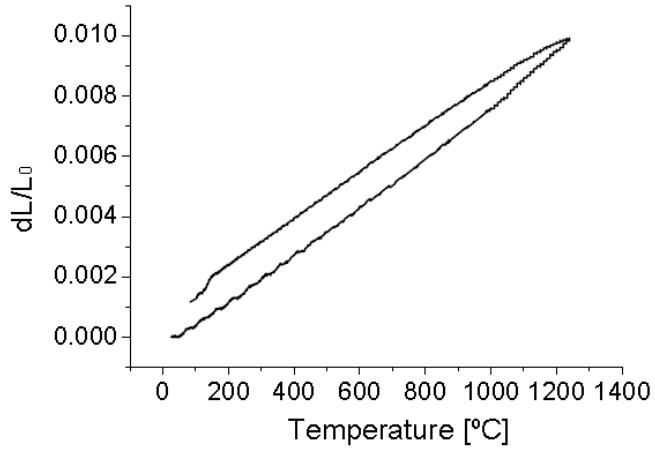

Fig. 2.12. Thermal strain evolution during a thermal cycle for the ATZ monolith. A linear trend is observed for heating and cooling steps [15].

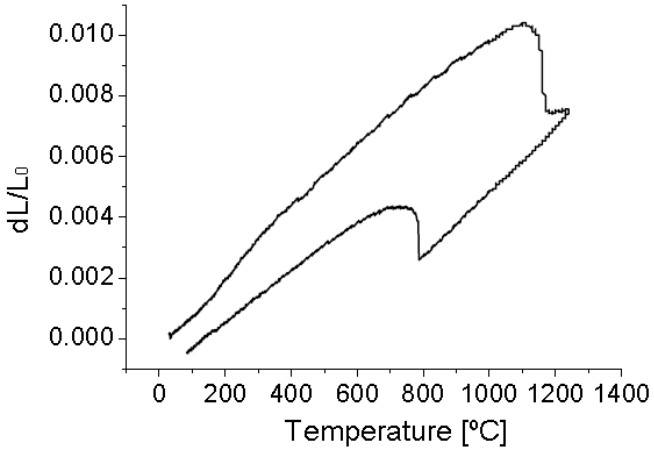

Fig. 2.13. Thermal strain evolution during a thermal cycle for the AMZ monolith. The change in slope, at temperatures about 725 ºC and 1150 ºC, is due to the zirconia phase transformation [15].

In Fig. 2.12 can be observed that the heating and cooling dilatometric curves show a linear behaviour with temperature (despite the small change in slope due to experimental uncertainties), suggesting that no microstructural changes take place during thermal cycling of the sintered ATZ compacts. In the case of AMZ monolith (see Fig. 2.13), the zirconia phase transformation from monoclinic to tetragonal during the heating step (at about 1150 ºC) and from tetragonal to monoclinic when cooling down (at about 725 ºC) is associated with a change in volume of the zirconia grains, which will condition the overall shrinkage of the AMZ monolithic compact. Fig. 2.14 shows the ATZ and AMZ cooling curves together.

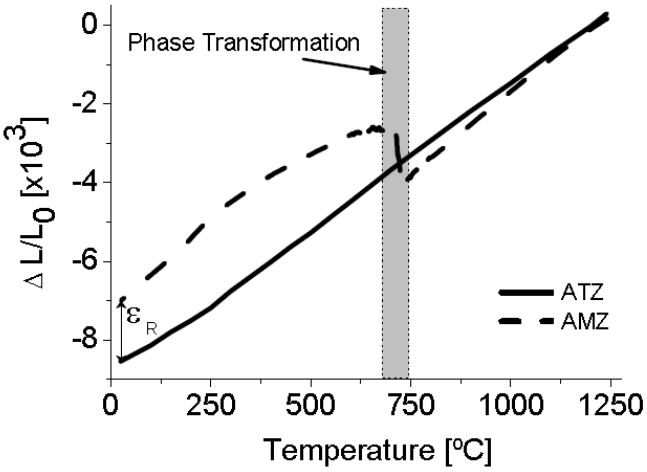

Fig. 2.14. Dilatometry curves between a reference temperature, i.e. 1250 ºC, and room temperature for the ATZ and AMZ monolithic materials. The change in slope on the AMZ curve is due to the zirconia phase transformation [15].

It can be observed in Fig. 2.15 the variation of the Young's modulus *E* for the ATZ and AMZ materials between room temperature and the reference one, i.e. 1250 ºC.

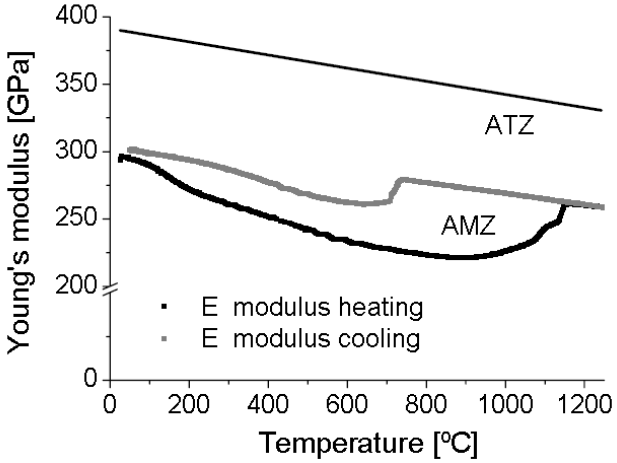

Fig. 2.15. Variation of the Young's modulus for the ATZ and AMZ materials with temperature. In the AMZ compact, the sudden change in slope at about 1150 ºC during heating and 725 ºC during cooling are due to the reversible phase transformation of the zirconia particles [15].

In the heating cycle, the Young's modulus of the AMZ decreases with temperature up to 1000 ºC, where the slope changes drastically due to the transformation of the zirconia particles, from monoclinic to tetragonal phase, in the range of 1000 – 1150 ºC. After the transformation, it retrieves its linear tendency with temperature. In the cooling cycle, the AMZ compact becomes stiffer with the decrease in temperature down to 725 ºC where a new zirconia phase transformation takes place, from tetragonal to monoclinic, in the range of 725 – 680 ºC. Below this temperature, the Young's modulus increases in a linear way until room temperature [15].

The fracture behaviour of multilayered laminates can be affected by residual stresses as related to strength and fracture toughness, and as referred to the fracture crack path. Compressive stresses usually oppose to crack growth [26], [27] and threshold strength can be developed [28]. The thin compressive layers are desirable for this reason, as they create an additional reinforcement besides diminishing the effective tension. When there are compressive stresses in the bulk (as for the AMZ layers), tensile stress exists there that is perpendicular to the layer at and near the surface, referred to as $\sigma_{yy,x}$ in work [15], as depicted schematically in Fig. 2.16.

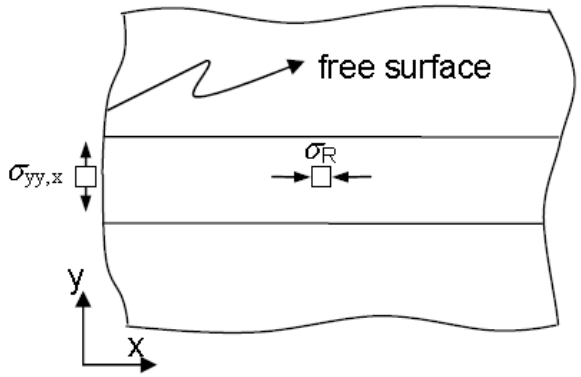

Fig. 2.16. Scheme of the stress components at the surface and in the bulk of a multilayered structure [15].

The stress $\sigma_{yy,x}$ is given by (2.6):

$$\sigma_{yy,x} = \frac{2}{\pi} * \left[\theta - \frac{1}{2}\sin 2\theta\right] * \sigma_R \tag{2.6}$$

where $\tan\theta = t/2x$, σ_R is the compressive stresses in the bulk.

The tensile stresses may induce crack extension. Because of that as written in [15] two situations must be considered:

"1) the extension of a pre-existing crack into the thin layer (termed "edging"), and 2), the growth of a crack of a certain depth (a) along the centreline of the thin layer (termed "channelling")".The equation for edge crack occurrence depends on the thin layer thickness and the magnitude of the residual compressive stress in it. The strain energy release rate function for a crack in this localized, tensile stress field is given by (2.7):

$$G = \frac{0.34\sigma_R^2(1-\nu^2)}{E} * t \tag{2.7}$$

where t, E and υ are the thickness, Young's modulus and Poisson's ratio.

From this condition, the critical thickness of the layer t_c above which edge cracking may occur, will be:

$$t_c = \frac{G_c * E}{0.34\sigma_R^2(1-\nu^2)} \tag{2.8}$$

As it was mentioned above, residual stresses at the free surface of a layered material are different from those within the bulk. The stress component is normal to the layer plane, $\sigma_{yy,x}$, and becomes significant when approaching the edges. Fig. 2.17 shows an edge crack experimentally in [15] observed running along the centre of a compressive layer of laminate.

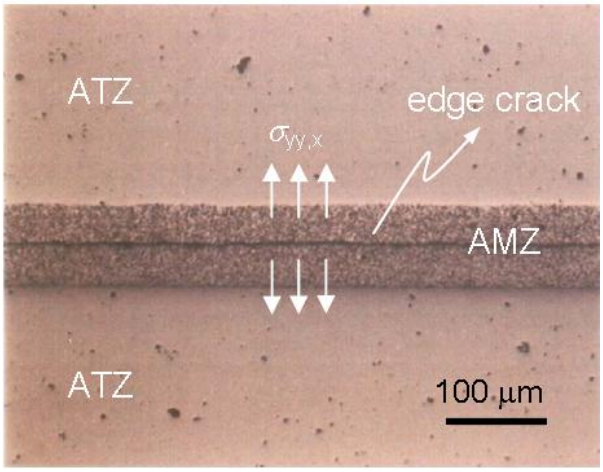

Fig. 2.17. Edge crack running along the centre of a AMZ compressive layer of a laminate [15].

2.2 Production

Ceramic layered materials are usually prepared by a regular alternation of at least two materials. Laminar structures allow combining various materials; the layers may be oriented differently so as to produce complicated macrostructure. Further processing of layered materials can be limited to several steps. The part is formed into the desired shape and further treatment, such as drilling holes, can be performed even before the sintering.

Almost all the methods have in common that the composite of individual layers is shaped in a so-called "raw" state (green body, before sintering). The laminate is created after subsequent annealing and sintering. The possible problems must be taken into account during manufacturing of the laminates, for example, mutual interaction of materials at the interface. This can be avoided by using systems that have limited mutual solubility and produces no intermediate phase - e.g. Al_2O_3 / ZrO_2 or Al_2O_3 / $Y_3Al_5O_{12}$ (YAG) [2]. Another problem is the different behaviour of different materials during sintering. If one material that constitutes the laminate sinters slower, the second material will be limited in sintering shrinkage. In the two-layered composite it can cause significant curvature or even fracture of the composite. In the case of a multilayer composite the curvature does not occur despite to the considerable residual tensions.

Basically, it is possible to make "raw" layers of different composition using almost all methods of ceramic processing. Depending on the shape of the sample and its thickness there are some methods that are better suited than others. The most common methods are tape casting, sequential slip casting, centrifugal casting and electrophoretic deposition [2].

2.2.1 Tape casting

This technique is widespread, which dates since the 60s of the last century. Laminates that are made by tape casting were used in the production of semiconductors in microelectronics. In 1973, first three-layered structural ceramics (Al_2O_3 / MgO-Al_2O_3) was made in this way [15].

Tapes of un-sintered ceramic are produced by tape casting (see the scheme in Fig. 2.18). They are laminated to each other in regular alternation (see Fig. 2.19) and subsequently at elevated temperature and pressure formed the "green body". Annealing and sintering result in strong bonding of layers. Samples that are prepared by tape casting have very sharp and straight interfaces [11]. This technique is widely used in the commercial production of electronic substrates and multilayer capacitors. Laminates were successfully manufactured in compositions of Al_2O_3/ZTA, Al_2O_3/ZrO_2, Al_2O_3/Al_2TiO_5, $MoSi_2$: $Al_2O_3/MoSi_2$ [11] and Al_2O_3/Ni [29] by using tape casting. Due to the difficult handling of thin tapes this method is suitable for layer thicknesses from 50 to 100 μm. Conversely thick layers can be formed simply by folding the same tapes at each other. Preparation takes a lot of time.

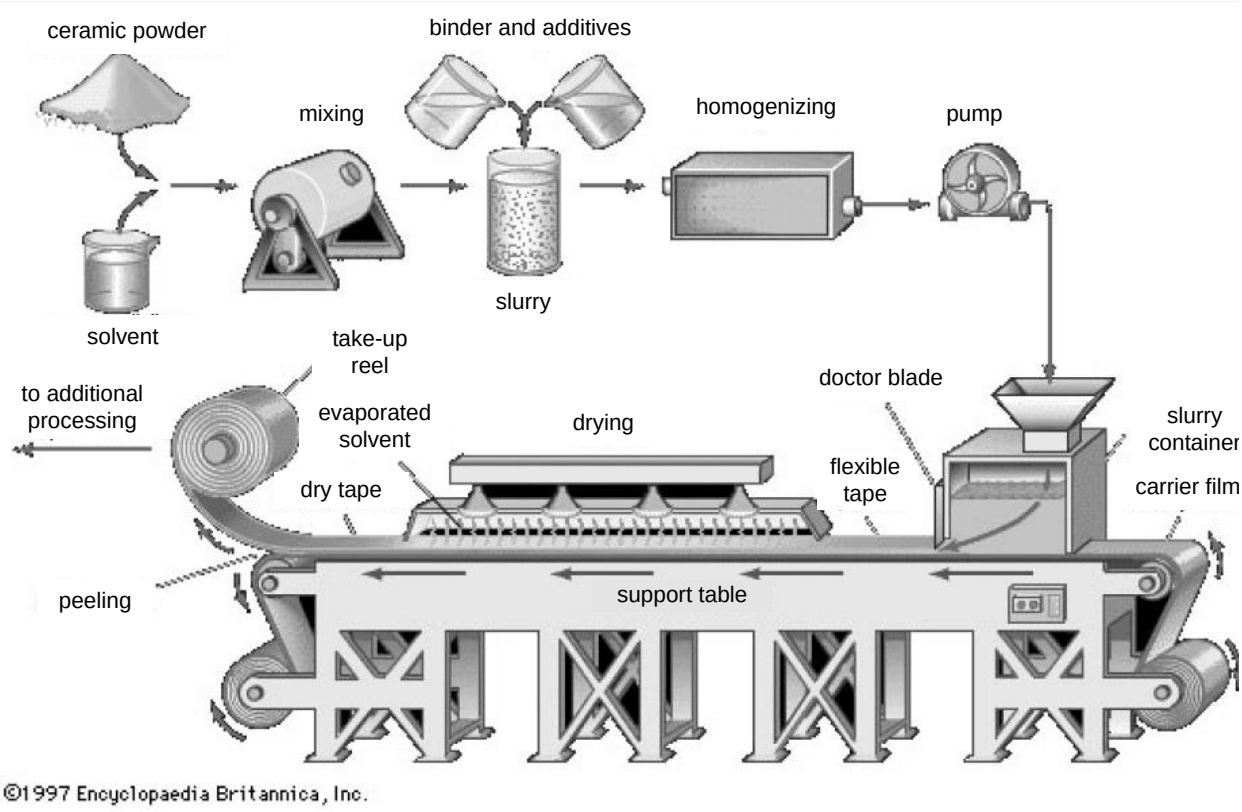

Fig. 2.18. Tape casting process [30].

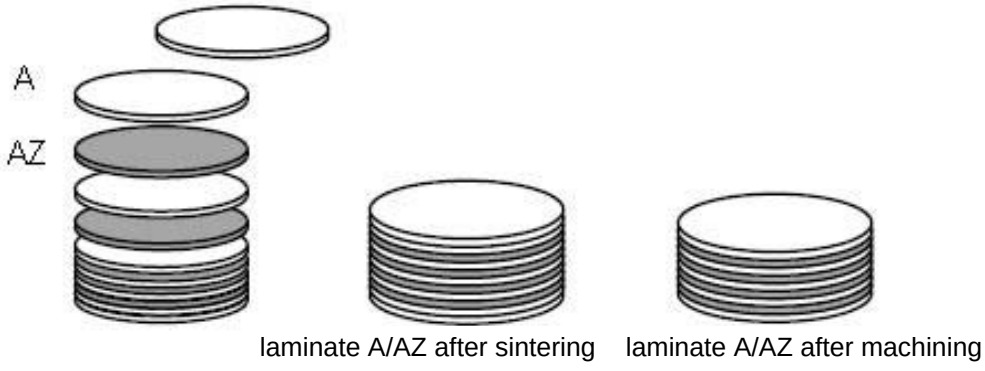

Fig. 2.19. Preparation of laminate by tape casting [31].

2.2.2 Sequential slip casting

The layered structure is formed by alternating casting of suspensions of different composition into the porous mold. Casting of individual layers is governed by kinetic curves that were calculated for each material. Equation for calculation of layer thickness is as follows [15]:

$$e^2 = k * t \tag{2.9}$$

where e is the wall thickness, k the kinetic constant and t the casting time.

First, an aqueous slurry is prepared from ceramic particles of submicrometers till micrometers in size and a small quantity of surfactant and organic polyelectrolytes. To obtain a good cohesion of the green body it is good to use slurry with a high proportion of solid phase (more than 60 wt. %) and very low viscosity (less than 40 mPa*s) [2], [15]. Close packing of particles leads to less shrinkage; consequently there is no tension, which could affect the final strength. The first of the slurry is then poured into a porous plaster mold, where it remains for a predetermined period that is determined from the kinetic curve casting. The liquid can be wicked away from the mold by pores (capillary pressure 0.1-0.2 MPa) [15]. The residue slurry is poured and the second slurry composition is poured on the first established layer. The process is repeated until the formed composite has a required number of layers. The material will remain in the form as long as shrinkage allows its removal. Outside of the mold the laminate is finally dried and subsequently sintered. In fact, the method is not so easy; time has to be compensated in depending on the number of layers. The thicker composite is the more time is needed for rise of water.

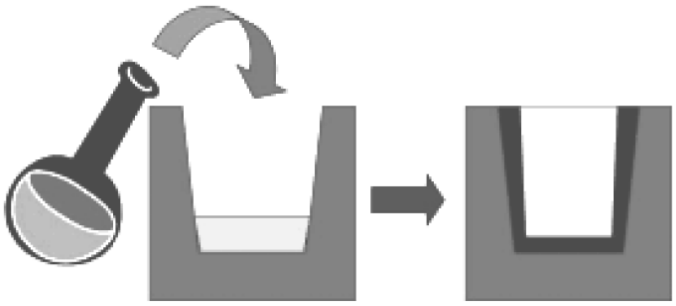

Fig. 2.20. Scheme of the sequential slip casting [15].

2.2.3 Centrifugal casting

This technique is younger and related to sequential molding, it is possible to produce composites with layers thickness from 10 μm [2], [12]. Pioneers of this method were Lange, Marshall et al [12], who found that by addition of an indifferent electrolyte (e.g. NH_4NO_3 or NH_3Cl) the interaction potential in high concentration can be adjusted. First, the aqueous acid suspension (pH 2) is prepared, in which between particles the repulsive electrostatic forces of long range are acting, so that particles are well separated and dispersed in suspension. After addition of indifferent salts the repulsive forces of short-range appear and reduce electrostatic forces that are between dispersed particles in the slurry. Weak attractive network of particles is created which prevents large segregation during centrifugation. Due to enough strong repulsive forces of short-range it is leading to high filling.

Depending on the required layer thicknesses the required amount of the colloidal aqueous suspension is poured to the cylindrical vessel, e.g. Teflon [12], [32], which contains

approximately 15 -20 vol.% of solid phase [32]. The container is then spun in a centrifuge (e.g. 800 rpm/min - 2 hours and 3000 rev/min - the last 5 min [32]). After centrifuging the supernatant (residual liquid) is removed and the second composition of slurry is placed into the container. The process is repeated until the laminate does not have the required number of layers (see Fig. 2.21). Subsequently, is recommended the established material to press or to shape, to dry and then to sinter in a composite.

The interface between lamellae is sharp, there is a rapid alternation of tensile and compressive internal stresses.

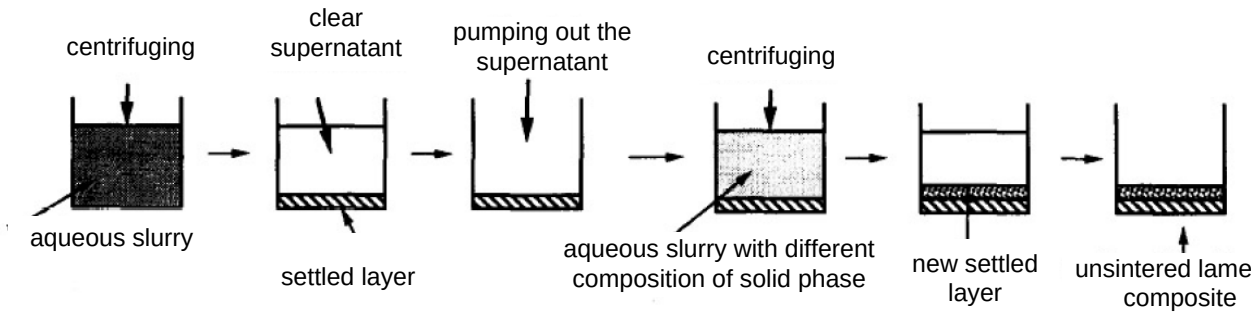

Fig. 2.21. Scheme of the centrifugal casting [32].

2.2.4 Electrophoretic deposition

The youngest, easy and relatively rapid technique for preparing layered ceramic materials. This method allows storage particles with size from nanometer to micrometer into layers of different shapes ranging from a few nanometers to several millimeters [20]. The typical layer thickness is from 1 to 3000 μm. The interface between layers is straight and well defined.

Electrophoretic deposition is based on the movement of charged ceramic particles in the DC electric field (= electrophoresis). A dense layer is formed by deposition of particles on oppositely charged electrode.

The key of achieving dense homogeneous body is the preparation of a stable colloidal suspension (avoid coagulation and sedimentation). In a liquid system with electrostatically stabilized ceramic particles, particles are enveloped by free ions which increase its density nearby particles and create an electric double layer. The stability of particles in the suspension is ensured due to the repulsive interactions between bilayers. Neutralization of surface charge arises on the electrode. Consequently, the concentration of ions in the electrode decreases, which changes the local pH of the slurry and due to Van der Waals forces, occurs to coagulation of the particles. [2]

Zhang derived formula (2.10) for the weight gain of the deposit over time. Assuming that in suspension occurs only to the deposition of particles, the kinetic equation can be written as follows [33]:

$$m = m_0 * (1 - e^{-\left(\frac{\mu * E_e}{d}\right) * t}) \tag{2.10}$$

where m_0 [kg] is the initial weight of the particles in the suspension, μ [m^2*V^{-1}] is electrophoretic mobility, E_e [$V*m^{-1}$] is electric field intensity, t [s] is time and d [m] is distance of the electrodes. Product $\mu * E$ represents the relationship for steady speed v of particles in suspension.

The quality of the deposit depends on many parameters such as intensity of electric field, the type, quantity and size of the powder; on the solvent and the stabilizer, deposition time, the distance of the electrodes, the dimensions of the cell etc.

Discoverers of application of EPD for creating layered ceramics were Sarkar, Nicholson et al. Laminar structure is achieved by moving the electrode between two different suspension. When an optimal thickness of the first layer is achieved, electrode is moved to a slurry with a different ceramic material. For a common deposition of different powders zeta potential must have the same polarity. Electrophoretic mobility should also be similar in order to achieve the homogeneous deposit.

EPD is suitable for the creation of structures with complex geometry. For example, these laminates were produced: Al_2O_3/ZrO_2 (stabilized with 3 mol% Y_2O_3) - (various shapes and thicknesses of the layers). [2], [20], [33], [34], [35], Al_2O_3 / Ni, $Al_2O_3/MoSi_2$, YSZ / Ni [35]; SiC/C [20].

2.3 Goals of the thesis

In this work ceramic laminates with layered architecture will be prepared by sequential slip casting and electrophoretic deposition. The laminates prepared will be tested on flexural strength. The structure of ceramic laminates will be examined and appearance of edge cracking will be evaluated. The relationship between the critical layer thickness of the compressive layer in which the edge cracking occur will be compared to results of the 2D finite element calculations. The crack propagation and crack bifurcation during flexural tests will be studied and effect of presence of edge cracking, formed due to high values of residual stresses, will be studied and compared.

3 EXPERIMENTAL PART

3.1 Raw materials

In the Fig. 3.1 are shown photos of Al2O3 and ZrO2 powders used for preparation of single-phase and two-phase depositions. The main characteristics of both powders are summarized in Table 3.1.

Table 3.1: Ceramic powders used for slip casting.

Material	Manufacturer	Indication of the manufacturer	Mean particle size (μm)	Density (g/cc)
Al_2O_3	Baikowski (France)	RC-HP-DBM	0.47	3,97
t-ZrO_2	Tosoh (Japan)	TZ-3YS-E Tetragonal phase	0.12	6,00
m-ZrO_2	Tosoh (Japan)	TZ-0 Monoclinic phase	0.10	5,88

High purity (liquid chromatography grade) water (Biosolve Chimie, France) was used as a dispersion medium for preparation the suspension of Al_2O_3 and ZrO_2 powders. Hydrochloric acid (99.9%, Penta, Czech Republic) or monochlor-acetic acid (p.a., Lachema, Czech Republic) was added to the suspension as a stabilizing and dispersing substance. In the case of slip casting preparation route the polyvinyl alcohol (fully hydrolyzed, Sigma-Aldrich, USA) was used as binder.

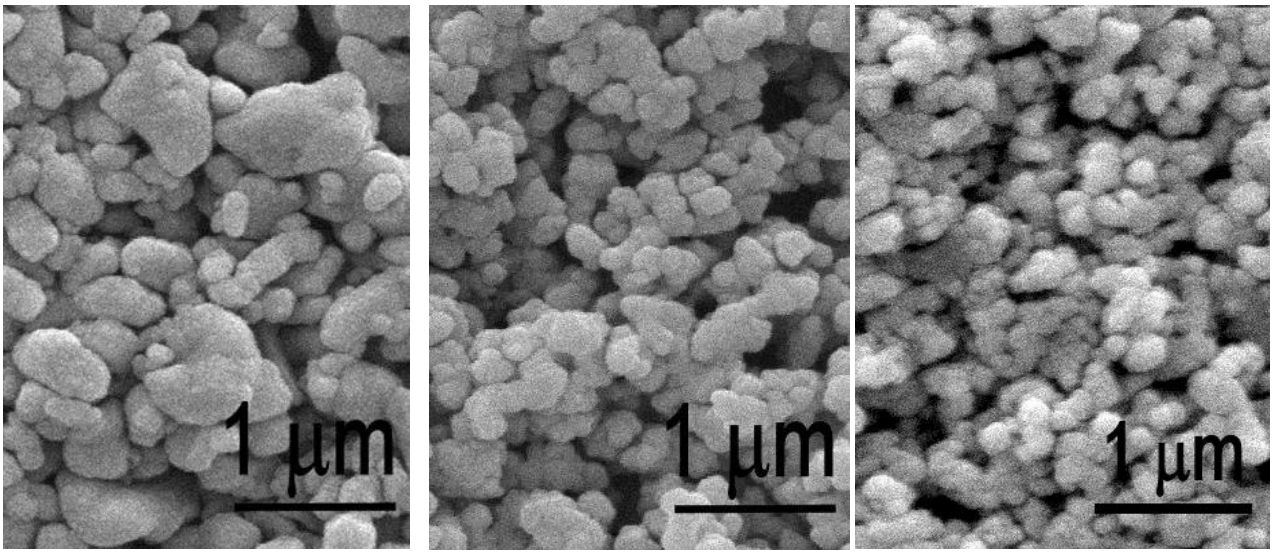

a) **b)** **c)**

Fig. 3.1. Photos of used powders of Al2O3 (a), t-ZrO2 (b) and m-ZrO2 (c).

3.2 Preparation of suspension

3.2.1 Preparation of suspension for sequential slip casting

In this work several slurries of 92,6% Al_2O_3 + 7,4% t-ZrO_2 (ATZ) and 60,5% Al_2O_3 + 39,5% m-ZrO_2 (AMZ) were prepared.

The weight of each part for 80g ATZ was calculated:

$$80g\ ATZ = 5{,}92g(\ tZrO_2) + 74{,}08g(\mathrm{Al_2O_3})$$

$$125g\ ATZ = 9{,}25g(\ tZrO_2) + 115{,}75g(\mathrm{Al_2O_3})$$

$$50g\ AMZ = 19{,}75g(\ mZrO_2) + 30{,}25g(\mathrm{Al_2O_3})$$

The slip preparation procedures are described as follows.

1) ATZ slip (in case of 7-layered ceramic laminates) 92,6% Al_2O_3 + 7,4% t-ZrO_2

From a 256 cc suspension, the solid content was fixed to 31,25%vol, i.e. the slip contained of 31,25 cc of ATZ and 68,75 cc of liquid phase. Liquid was contained of 176 ml of (DI) water with 0,88 g of polyvinyl alcohol (PVA). The ratio water – PVA was selected as 200:1, respectively. After achieving of the homogeneity of obtained liquid phase, the hydrochloric acid (HCl) was added as the stabilizing and dispersing agent in ratio of 1ml per 100 ml of liquid. The liquid phase was magnetically stirred by device Heidolph MR Hei-Tec (Heidolph Instruments, Germany). After complete mixing of the liquid, 80g of ATZ powder was added. Then liquid with powder were good stirred and the desired suspension was stirred in an ultrasonic bath Elma S30 (Elmasonic, Germany) in order to dispersion of any potential agglomerate.

2) AMZ slip (in case of 7-layered ceramic laminates) 60,5% Al_2O_3 + 39,5% m-ZrO_2

Suspension with AMZ content was prepared similarly to the suspension with ATZ case. 160 cc suspension contained of solid content fixed to 31,25 %vol. and 68,75 cc of liquid phase, i.e. 110 ml of (DI) water with 0,55 g of PVA mixed with 1,1 ml HCl. Then the magnetic stirrer and an ultrasonic bath, as well as in case of ATZ, were used for stirring 50g of AMZ powder in obtained liquid.

3) ATZ slip (in case of 9-layered ceramic laminates) 92,6% Al_2O_3 + 7,4% t-ZrO_2

Steps of preparation of ATZ suspension for 9-layered ceramic laminates were the same to preparation of ATZ suspension for 7-layered ceramic laminates. Only amounts of contents of liquid and solid phases are different as follows.

360 g of suspension was prepared:

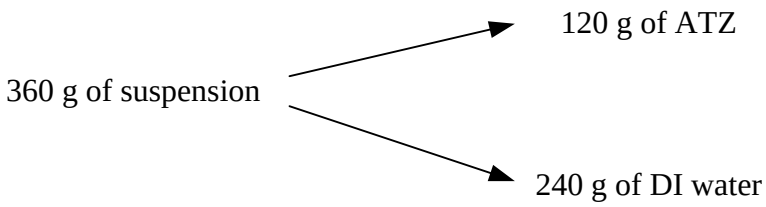

120 g of ATZ contained of:

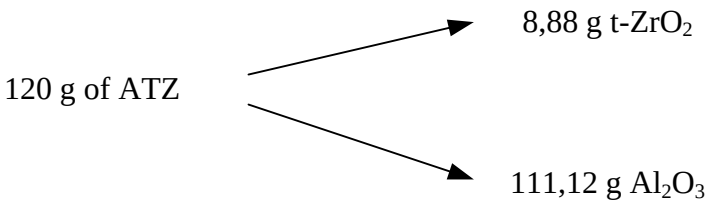

As well as in the case of ATZ suspension for 7-layered ceramic laminates, 3,6 ml HCl and 1,8 ml PVA were added. The final ATZ suspension contained:

$$360\ g\ ATZ\ suspension \begin{cases} 111{,}12\ g\ Al_2O_3 \\ 8{,}8\ g\ t-ZrO_2 \\ 120\ g\ H_2O\ (DI) \\ 3{,}6\ ml\ HCl \\ 1{,}8\ ml\ PVA \end{cases}$$

4) AMZ slip (in case of 9-layered ceramic laminates) 60,5% Al_2O_3 + 39,5% m-ZrO_2

The preparation of AMZ suspension for 9-layered ceramic laminates was the same to preparation of AMZ suspension for 7-layered ceramic laminates. The amounts of contents of liquid and solid phases are shown as follows:

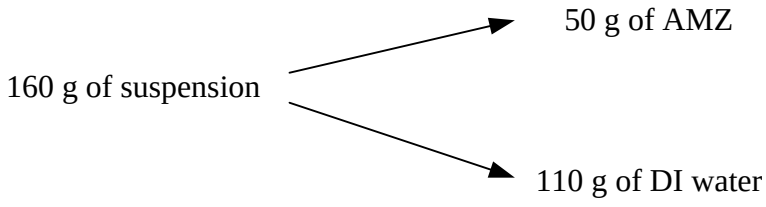

50 g of AMZ contained of:

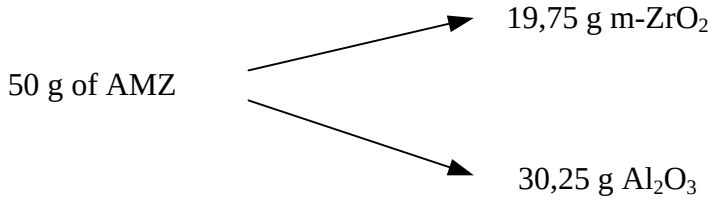

Also 1 ml HCl and 0,5 ml PVA were added to AMZ suspension. The final AMZ suspension contained:

$$160\ g\ AMZ\ suspension \begin{cases} 30{,}25\ g\ Al_2O_3 \\ 19{,}75\ g\ mZrO_2 \\ 110\ g\ H_2O\ (DI) \\ 1\ ml\ HCl \\ 0{,}5\ ml\ PVA \end{cases}$$

3.2.1 Preparation of suspension for sequential electrophoretic deposition

For electrophoretic deposition the suspensions were prepared in the same manner as for slip casting. Just the portion of powder in the suspension was lowered to 15 wt.% because the electrophoretic deposition process used diluted suspension. The suspensions were prepared by mixing 15 wt.% of ATZ or AMZ powder mixture powder in 85 wt.% of isopropanol (i.e. 15 wt.% of powder, 12.75 wt.% of monochloracetic acid and 72.25 wt. % of isopropanol).

1) ATZ slip 92,6% Al_2O_3 + 7,4% t-ZrO_2

256 g of suspension was prepared for 7-layered ceramic laminates (for 9-layered ceramic laminates was the same):

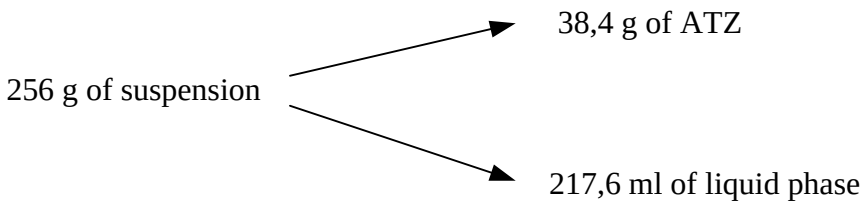

38,4 g of ATZ contained of:

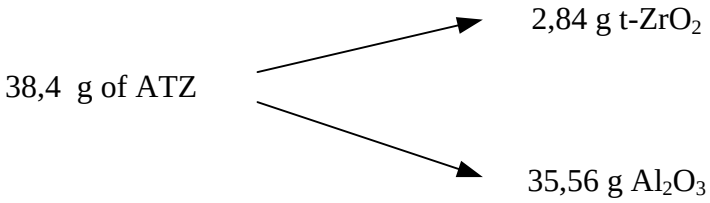

217,6 ml of liquid phase consisted of 32,64 ml $C_2H_3ClO_2$ and 184,96 ml C_3H_8O. The final ATZ suspension contained:

$$256\ g\ ATZ\ suspension \begin{cases} 35{,}56\ g\ Al_2O_3 \\ 2{,}84\ g\ t-ZrO_2 \\ 32{,}64\ \ ml\ C_2H_3ClO_2 \\ 184{,}96\ ml\ C_3H_8O \end{cases}$$

2) AMZ slip 60,5% Al_2O_3 + 39,5% m-ZrO_2 (for 7-layered and 9-layered ceramic laminates)

200 g of suspension was prepared for 7-layered ceramic laminates (for 9-layered ceramic laminates was the same). The amounts of contents of liquid and solid phases are shown as follows:

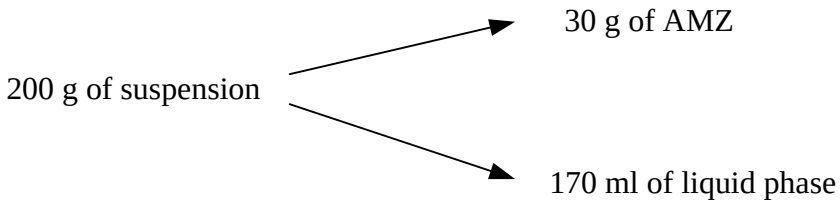

30 g of AMZ contained of:

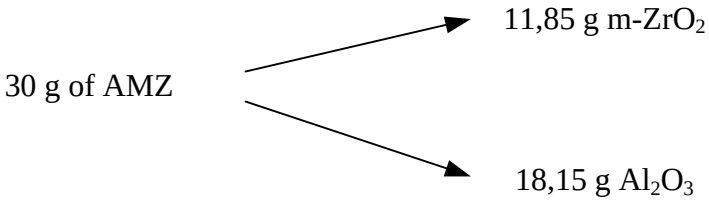

170 ml of liquid phase consisted of 25,5 ml $C_2H_3ClO_2$ and 144,5 ml C_3H_8O. The final AMZ suspension contained:

$$200\ g\ AMZ\ suspension \begin{cases} 18{,}15\ g\ Al_2O_3 \\ 11{,}85\ g\ m-ZrO_2 \\ 25{,}5\ ml\ C_2H_3ClO_2 \\ 144{,}5\ ml\ C_3H_8O \end{cases}$$

Finally, ATZ and AMS suspensions were ready for casting of them into the mould.

3.3 Sequential slip casting

In this method a suspension composed of micrometer and submicrometre size of the ceramic particles in the liquid was poured into a silicone mold containing the cylinder of plaster (see Fig. 3.2). The capillary suction pressure of ≈ 0.1 – 0.2 MPa is provided by porous nature of the mold, allowing the liquid from the suspension to be drawn into the plaster base of the mold [3].

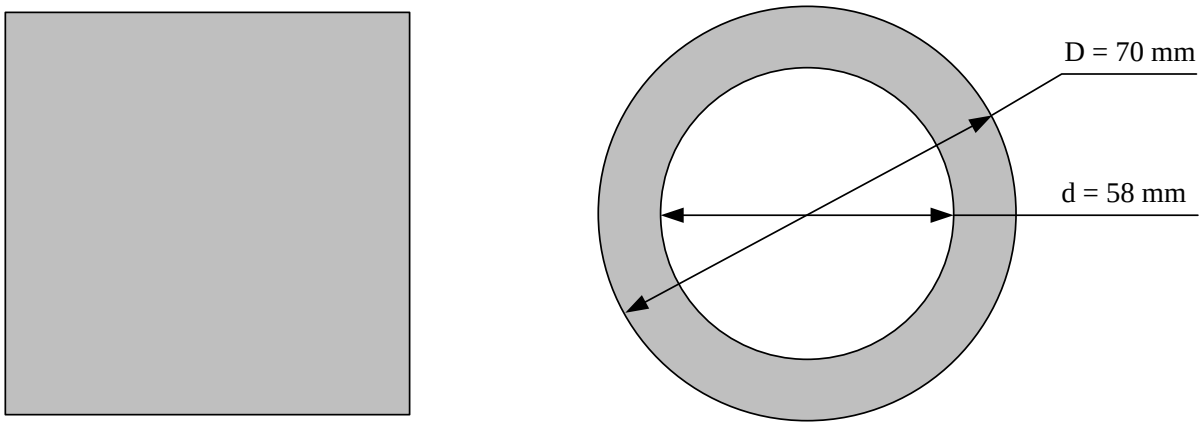

Fig. 3.2. Slip cast mould with porous plaster insert.

It is also required the use of the slurries with high content of solid particles in order to achieve good compact and green density. Under these conditions, and as a consequence of increased degree of packing between the particles, the shrinkage of the part will be lower during drying. Thereby, stresses that might influence to the final strength of the sample do not develop at a significant level. On the other hand, viscosity is another important factor that has to be taken into account in the preparation of slip casting. The more liquid is the slurry the better it is distributed over the mould, reaching a good dispersion and homogeneity [15].

Ceramic laminates were casted layer by layer from prepared suspensions, which are described above. Depending on the desired thickness of each layer the certain amount of the suspensions was poured into the mould. Time of casting of each 7 layered and 9-layered laminates were ≈5 days and ≈7 days respectively. In Table 3.2 the prepared layered composite materials are listed.

Table 3.2: Layered composite materials prepared by slip casting method.

Designation	Type of sample	Phase composition
Lam V5A SC	Multi-component layered	ATZ/AMZ
Lam sym A SC	Multi-component layered	ATZ/AMZ
Lam V3A SC	Multi-component layered	ATZ/AMZ
Lam V5B SC	Multi-component layered	ATZ/AMZ
Lam sym B SC	Multi-component layered	ATZ/AMZ
Lam V3B SC	Multi-component layered	ATZ/AMZ

Casted laminates were dried in stove Venticell (BMT MMM Group) at gradually increasing temperature from 36℃ until easy separation them from plaster bottom. Then they were annealed (800℃ for 1 h) and sintered (1550℃ for 2 h) in the air atmosphere.

3.4 Sequential electrophoretic deposition

Electrophoretic deposition was performed in a horizontal electrophoretic cell (the direction of movement of particles during deposition is going in the horizontal plane). 80 ml of suspension was placed into a glass vessel of electrophoretic cell. Two electrodes made of stainless steel with polished surface were placed into a cell with suspension. The distance between the electrodes was 26 mm and the effective area of the electrode that was immersed to the slurry was 18,7 cm^2. Schematic sectional view of used electrophoretic cell is shown in Fig. 3.3.

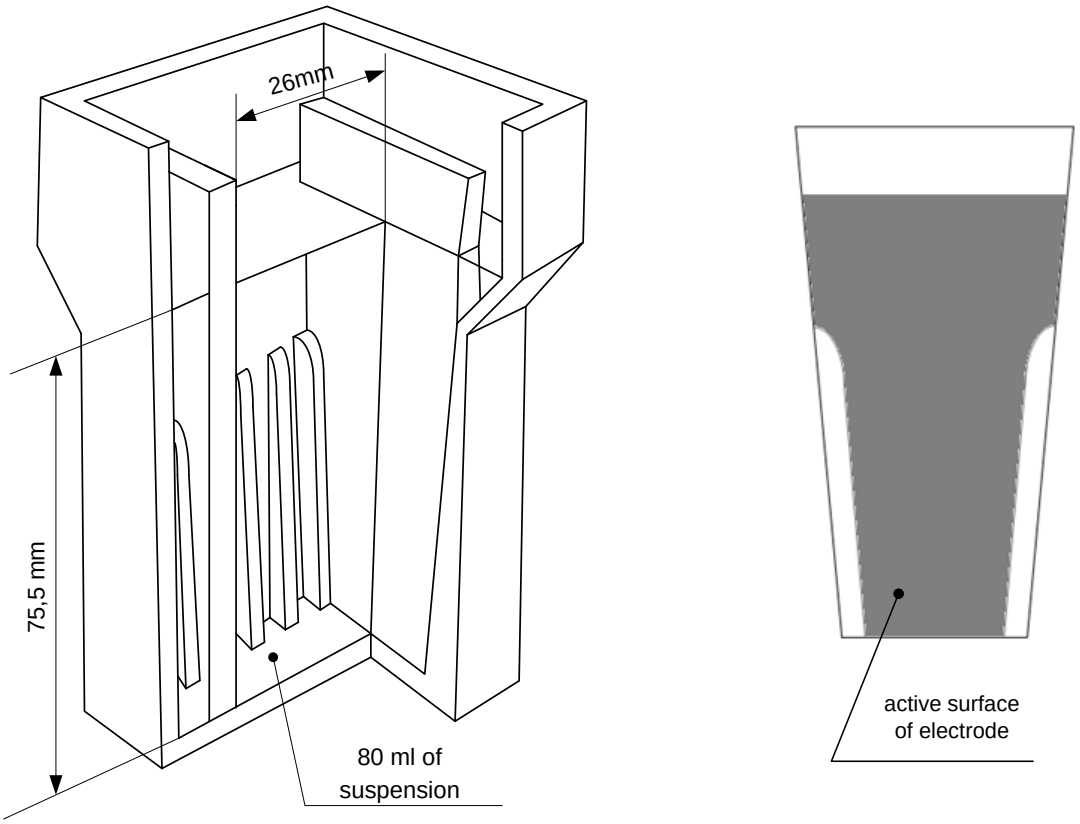

Fig. 3.3. Schematic sectional view of used cell for electrophoretic deposition for ceramic materials [36].

The figure shows the trapezoidal shape of the active surface of the electrode. The wiring diagram of devices during electrophoretic deposition is shown in Fig. 3.4.

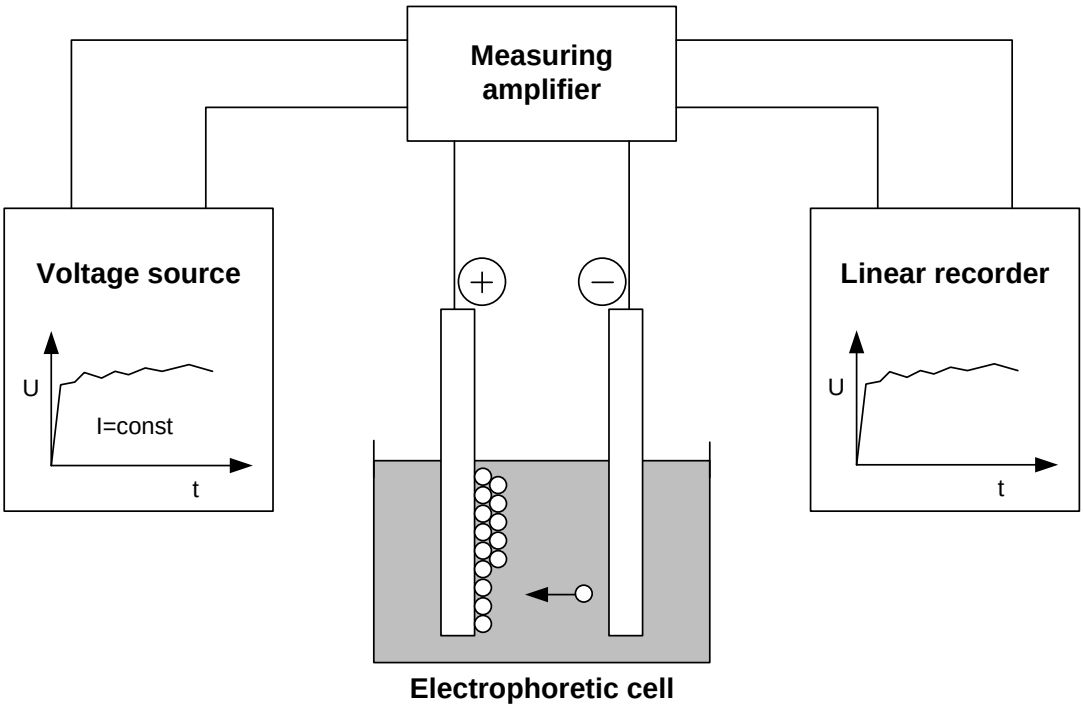

Fig. 3.4. The wiring diagram of experimental devices during the electrophoretic deposition of ceramic materials [36].

Electrophoretic deposition was carried out at a constant current of 5 mA. Microcomputer controlled stabilized DC voltage source was used as a constant current source (E815, Consort, Belgium). Suspension was stirred during electrophoretic deposition due to the particle sedimentation. As seen from the results listed in the work [34], there is a sedimentation of particles to the bottom of the cell during the electrophoretic deposition. Deposition was always interrupted to avoid damaging of the surface of the deposited layer, or to reduce compactness of layers that are created by poor deposition of particles in flowing liquid; the electrodes were removed from the suspension and then the suspension was mixed. All the deposits together with the electrodes were dried at room temperature for 24 h and then removed from the electrode and annealed and sintered in the same manner as slip casted laminates.

In Table 3.3 the prepared layered composite materials are listed.

Table 3.3: Layered composite materials prepared by electrophoretic deposition.

Designation	Type of sample	Phase composition
Lam V3/9 EPD	Multi-component layered	ATZ/AMZ
Lam V5/7 EPD	Multi-component layered	ATZ/AMZ
Lam V3/7 EPD	Multi-component layered	ATZ/AMZ
Lam SymP2/9 EPD	Multi-component layered	ATZ/AMZ

3.5 Preparing of samples for testing of the mechanical properties

Sintered samples were prepared by standard ceramographic methods. The samples were cut to pieces by ISOMET 5000 linear precision saw (Buehler, USA). From slip casted laminates the bars having cross section ca 10x40 mm were cutted. From laminates prepared by electrophoretic deposition the samples having cross section dimensions ca 4x30 mm were prepared.

3.6 Mechanical testing

An Instron 8862 (UK) universal testing system with threepoint fixtures having span of 40 mm and 16 mm was used for the flexural strength measurement of slip-casted and electrophoretically deposited samples, respectively. The cross-head speed of 0.5 mm min^{-1} was applied according to requirements given in the standard [37]. Flexural strength values were calculated from the fracture (maximum) force and dimensions measured prior to the test.

3.7 Preparing of samples for edge cracks observation

Then samples of laminates prepared were pressed into resin by equipment Opal 410 (made in Germany). Grinding of the samples was performed on equipment STRUERS LaboForce-3 LaboPo-5 (made in Denmark) with using diamond discs and pastes up to size 1 μm.

3.8 Edge cracks observation

The thickness of layers (used for residual stresses calculation) and edge cracks observation was performed using OLS 3100 confocal microscope (Olympus, Japan).

4 RESULTS AND DISCUSSION

4.1 Analysis of prepared laminates

The slip casting and electrophoretic deposition methods were used for production of ceramic laminates of different compositions (preparing is described in the previous chapter). Six samples of ceramic laminates were prepared by using slip casting and four samples were prepared by EPD. As it is seen on Fig. 4.1 samples consisted of layers of different content with different layer thickness (see Table 4.1). Thicknesses presented in Table 4.1 were obtained as average from minimally 10 independent measurements using calibrated laser confocal microscope. Also it is clearly seen that structure of the laminate prepared by EPD has porosity, but porosity of structure of ceramic laminates prepared by slip casting is much more pronounced. Small particles of the material can be seen in the figures, perhaps it is due to the large size of some of the particles of raw powder or it is related to insufficient time of stirring two different materials, which was not enough to dissolve some of the agglomerated particles.

The Fig. 4.1a and Fig. 4.1b also demonstrate that the clean and straight interfaces between ATZ and AMZ layers were obtained in the production of laminated ceramic materials.

a) 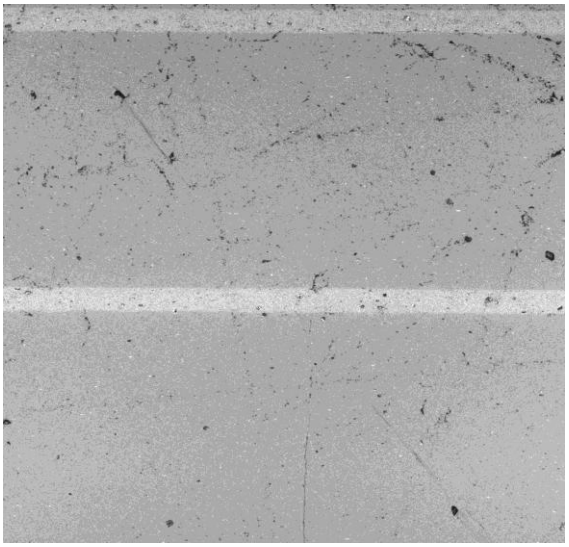 b) 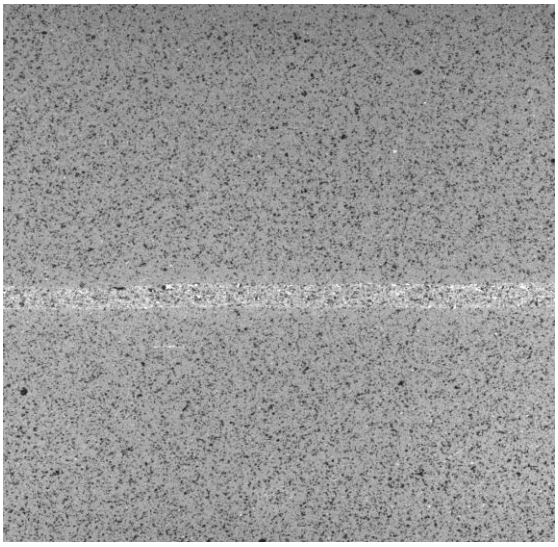

Fig. 4.1. Microstructure of prepared samples by EPD (a) and slip casting (b) of ceramic laminates after sintering (bright colour – AMZ layers; dark colour – ATZ layers).

In addition it should be noted that in some laminates the delamination was observed along the interface between layers of two different materials (see Fig. 4.2). Delamination can be related with different values of the residual stresses generated during cooling after sintering due to the different coefficients of thermal expansion. These residual stresses can be released due to presence of pores and/or other inhomogeneities.

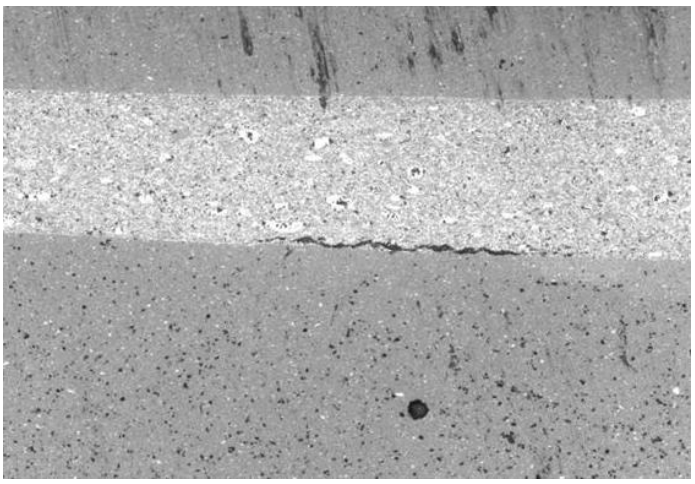

Fig. 4.2. Delamination between ATZ and AMZ layers of laminate Lam V3A (slip casted).

Table 4.1. Layer thickness of prepared ceramic laminates.

		Layers thickness [mm]								
		ATZ	AMZ	ATZ	AMZ	ATZ	AMZ	ATZ	AMZ	ATZ
Slip casting	Lam SymA	0.887	0.029	1.098	0.022	0.951	0.076	1.281	0.069	1.223
	Lam V3A	0.130	0.181	1.592	0.050	1.583	0.0193	1.483	0.107	0.082
	Lam V5A	0.025	0.167	1.669	0.038	1.670	0.039	1.764	0.141	0.049
	Lam SymB	0.811	0.287	0.757	0.221	0.845	0.318	0.739	-	-
	Lam V3B	0.201	0.303	1.192	0.082	1.194	0.277	0.258	-	-
	Lam V5B	0.059	0.291	1.432	0.092	1.527	0.586	0.073	-	-
EPD	Lam V3/9	0.158	0.262	0.615	0.054	0.608	0.057	0.661	0.309	0.185
	Lam V5/7	0.038	0.268	0.737	0.056	0.773	0.290	0.036	-	-
	Lam V3/7	0.103	0.265	0.992	0.111	0.981	0.302	0.181	-	-
	Lam SymP2/9	0,497	0,198	0,483	0,194	0,465	0,185	0,448	0,169	0,420

4.2 Residual stresses

As it is known from Chapter 2 ceramic laminates consisted of layers from different materials. Due to thermal expansion mismatch between layers the residual stresses developed in the individual layers during cooling from sintering temperature. Residual stresses of prepared ceramic laminates were calculated by using web-application "Laminate theory (web-App) [38] released by Institut für Struktur- und Funktionskeramik - Montanuniversität Leoben, 15.01.2012

(Austria). This application is based on Hook's law of the single layer, condition of the stress and movement equilibrium over the laminate height, and on the global behaviour of laminate under given boundary conditions [39].

For calculation residual stresses some material properties were required, as follow:

- volume thickness of AMZ layers [mm],
- volume thickness of ATZ layers [mm],
- total laminate height [mm],
- properties of materials such as Young's modulus and Poisson's ratio:

Material	Young's modulus [GPa]	Poisson's ratio
AMZ	280±10	0.22
ATZ	390±10	0.22

- temperature increment ΔT.

The temperature increment was chosen as $\Delta T = 1250℃$ as in work [15] because conditions and properties of the materials in that work were close and similar to the all conditions and material properties of this investigation. Calculated values of residual stresses are given in the Table 4.2 below.

Table 4.2. Residual stresses in compressive AMZ layers.

Ceramic laminate prepared by slip casting	Residual stress σ_{res} [MPa]	Ceramic laminate prepared by EPD	Residual stress σ_{res} [MPa]
Lam SymA	-719	Lam V3/9	-431
Lam V3A	-652	Lam V5/7	-403
Lam V5A	-650	Lam V3/7	-433
Lam SymB	-454		
Lam V3B	-472	Lam SymP2/9	-424
Lam V5B	-428		

High values of residual stresses in the compressive AMZ layers may contribute to the formation of edge cracks at the free surface, which propagate in-plane of AMZ layer. Edge cracking is described in detail in the next chapter.

4.3 Edge cracks

In this investigation the model of edge crack formation and propagation in ceramic laminates developed by Sevecek at al. [40] was applied to compare the obtained results with results obtained in work [40]. This 2D parametric numerical model of finite element (FE) has been developed to assess the effect of residual stress and compressive layer thickness on the formation of edge crack. Authors of that work used the stress-energy coupled criterion (CC) to predict the formation and propagation of the edge cracking [40].

4.3.1 Modeling of edge crack formation and propagation

The model was developed based on research conducted on ceramic laminate that consists of 9 alternated layers composed of two different materials: ATZ (alumina with 5% tetragonal zirconium) and AMZ (alumina with 30% monoclinic zirconium). Schematic of a prismatic bending bar with sizes of $(L \times B \times H)$ $45mm \times 4mm \times 3mm$ is shown on Fig. 4.3 [40].

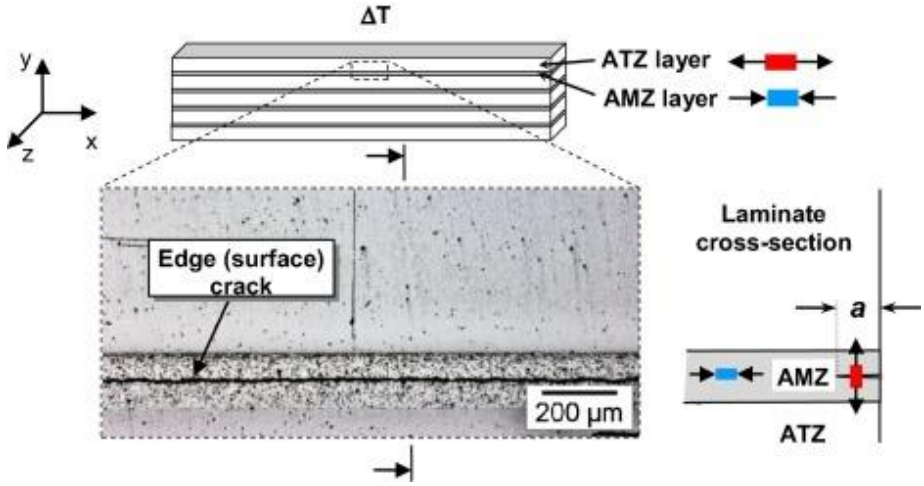

Fig. 4.3. Experimental observation of the edge crack phenomenon in a compressive AMZ layer, and stress redistribution at the free surface of the thin compressive layer [40].

Fig. 4.3 shows an edge crack in the center of AMZ layer. It is associated with the presence of compressive stresses in the AMZ layer. These residual stresses occur in the layers of the laminate during the cooling process from the sintering temperature. The compressive stresses occur in AMZ layer, and the tensile stresses occur in ATZ layer. Thickness of the AMZ layers of the laminate varied from 30μm to 350μm, which could lead to different levels of residual stress [40].

The authors which developed the given model used the FE software ANSYS 15.0 for numerical calculations. They calculated the actual potential energy of the cracked body $W(a)$ and used the obtained value for the calculations of the incremental energy release rate $G_{inc}(a)$ and for the energy release rate (ERR) $G(a)$ at the tip of crack as below:

$$G_{inc}(a) = -\frac{W(0) - W(a)}{a}$$
$$G(A) = -\frac{dW(a)}{da} \quad (4.1)$$

where, W(0) is the potential energy of the uncracked body [40].

Further, in order to determine the appropriate conditions for the occurrence of edge cracking, they used a stress-energy coupled criterion, which claims that the edge cracks occur if two conditions are performed simultaneously:

$$G_{inc}(a) \geq G_c(AMZ) \text{ and } \sigma_{yy} \geq \sigma_c(AMZ) \quad (4.2)$$

where, σ_c is the critical tensile stress, $\sigma_{yy}$is the stresses along the prospective crack path. The first condition says that there must be enough energy available to create cracks; the second condition indicates that the tensile stress should be higher than the tensile strength of the material along the entire length of the intended crack. They assumed that the crack appears almost simultaneously around the sample, and then begins to grow deeper [40].

The authors of [40] applied the criterion the stress energy in ceramic laminates, thus they described the formation of edge cracks in laminates with a layered architecture (see Fig. 4.4) with layer thickness of AMZ $t = 150\mu m$ [40].

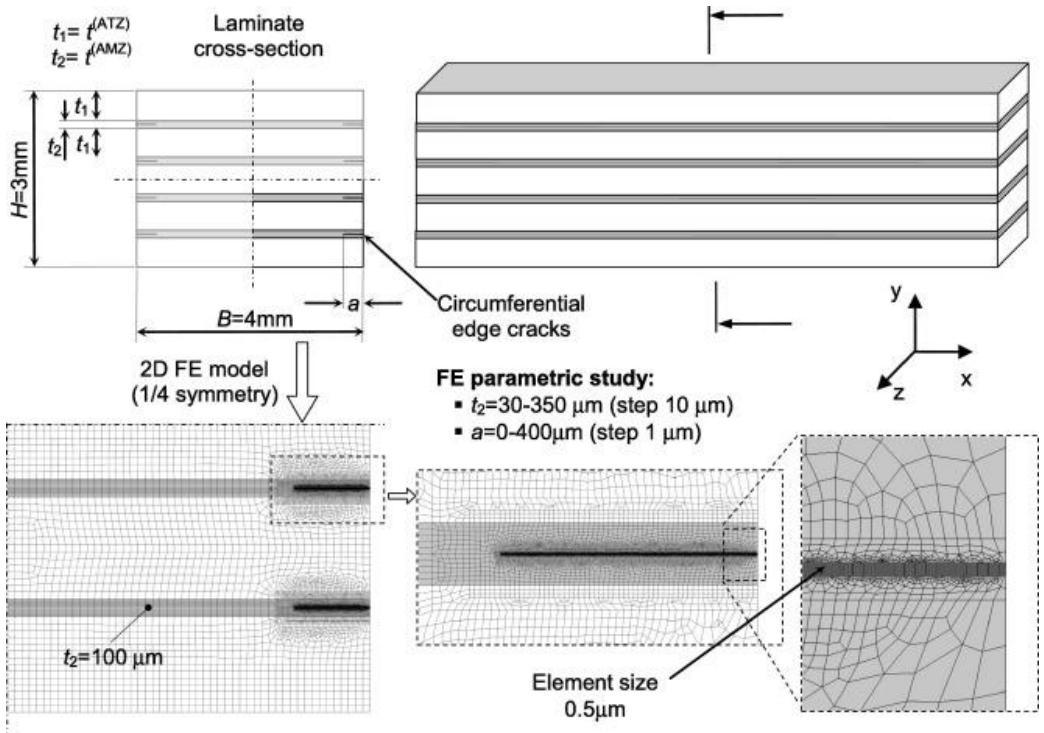

Fig. 4.4. Schematic of the fully parametric FE model, developed to study the propagation of edge cracks in the compressive AMZ layers [40].

Value of compressive residual stresses increases during cooling of the sample, i.e. due to temperature changes ΔT from the sintering temperature. They also described the formation of edge cracks at different values of compressive residual stress and determined that if the level of compressive residual stress increases up to a value σ_{res}(AMZ) =300 MPa, there edge crack occurs in the AMZ layer that is thicker than 222 μm, because both conditions (4.2) are satisfied; and at a AMZ layer thickness lower than 222 μm – no edge cracks are predicted. Beyond the critical layer thickness t_c =307μm the crack propagates along the AMZ layer that leads to total delimitation of the ceramic laminate [40].

The combined effect of compressive residual stresses σ_{res}(AMZ) and thickness of AMZ layer t(AMZ) on final depth of edge crack, as it is predicted in investigation, is shown on Fig. 4.5 [40].

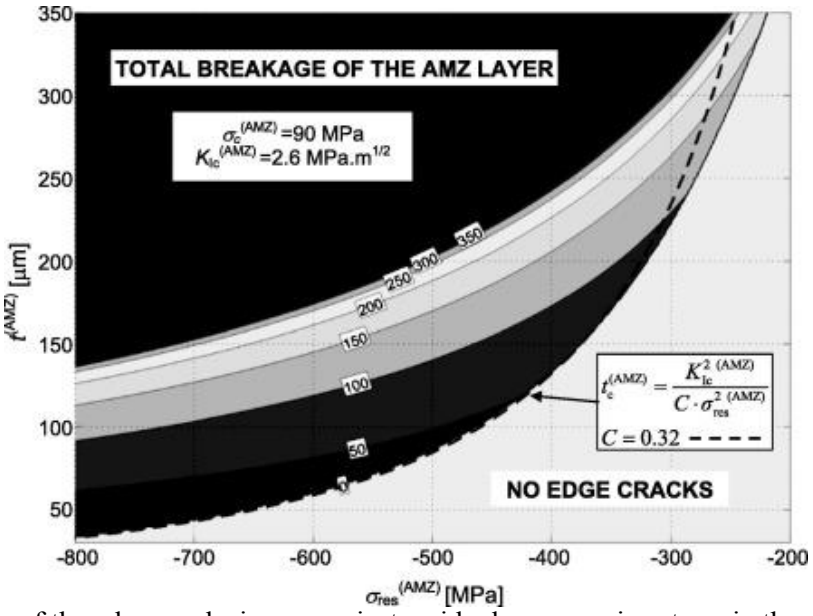

Fig. 4.5. Depths of the edge cracks in µm against residual compressive stress in the AMZ layer and thickness of the compressive layer. The numbers in white boxes inside the plot denote the final edge crack depth in µm for certain combination of σ_{res}(AMZ) and t(AMZ) [40].

The residual stress varies in the interval from -200 MPa to -800 MPa and thickness of AMZ layer ranges from 30 μm to 350 μm in the Fig. 4.5. The depicted curves allow assessing the crack depth. Thereby the using of respective values of residual stresses in compressive AMZ layers and their thickness t(AMZ) gives the opportunity to determine if the edge cracks exist in certain AMZ layer. If such combination lays in light-grey area it means that in that layer there are no edge cracks. If the combination of σ_{res}(AMZ) and t (AMZ) is in the centre part of the graph - the edge cracks are expected. And finally the pair of combination σ_{res}(AMZ) and t (AMZ) can lead to breakage of AMZ layer if it lays in dark grey part in the top of graph [40].

The layer thickness, which leads to the appearing of edge cracking, can be described using the following equation derived by Ho and Hillman in work [41]:

$$t_c(AMZ) = \frac{K_{IC}^2(AMZ)}{C * \sigma_{res}^2(AMZ)} \tag{4.3}$$

where, K_{IC} is the fracture toughness of AMZ layer, σ_{res} is the residual stress in compressive AMZ layer and *C* is constant that was estimated by authors of work [41] to be equal to 0,34 and authors of work [40] calculated it by using CC approach and Eq. (4.3) and obtained a similar result for C constant as $C = 0{,}32$ [40].

The black thin dotted line in Fig. 4.5 is represented to the critical layer thickness on the level of residual stress σ_{res}(AMZ) [40].

4.3.2 Edge cracks in prepared ceramic laminates

Prepared ceramic laminates were studied by laser confocal microscope. Edge cracks were found in some compressive AMZ layers as it can see in Fig. 4.6 and Fig. 4.7.

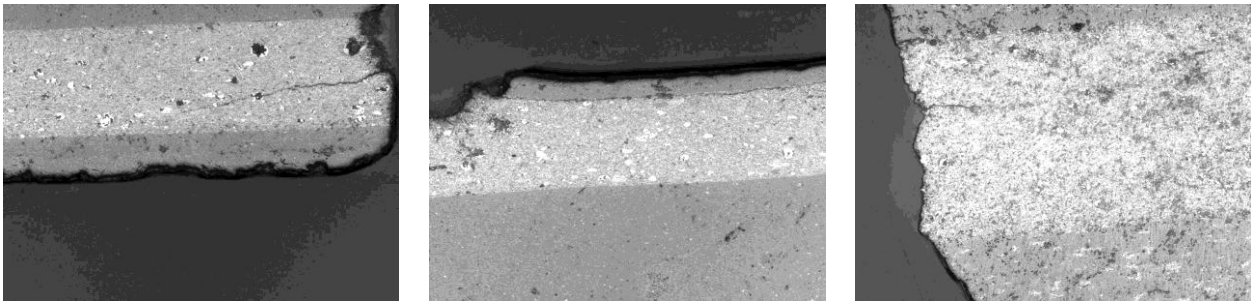

Fig. 4.6. Edge cracks in prepared ceramic laminates by slip casting method.

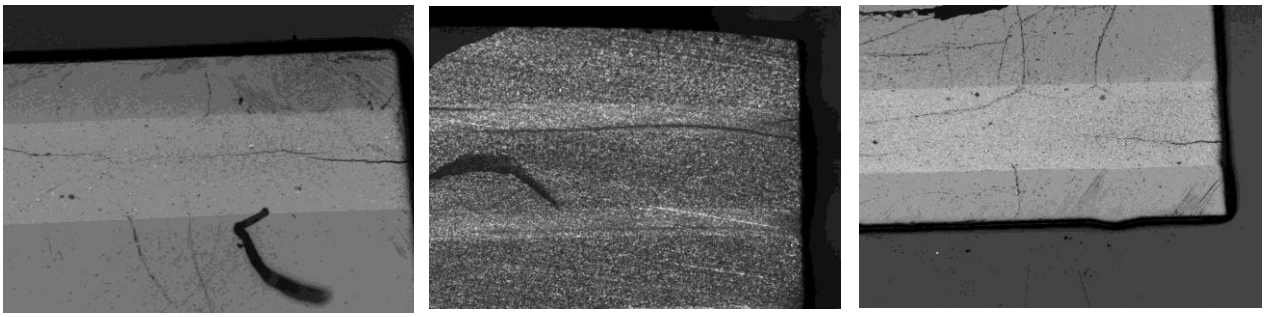

Fig. 4.7. Edge cracks in prepared ceramic laminates by EPD.

From the given pictures it is clearly seen that edge cracks appear from the edge of AMZ layer and propagate deep in-plane AMZ layer without crossing the interface with ATZ layer.

However, edge cracks were found not in each AMZ layer. Table 4.3 and Table 4.4 show the results of detection of edge cracks in each AMZ layer of ceramic laminates prepared by slip casting and EPD.

The Table 4.3 shows that the predicted model developed by authors of the work [40] the presence or absence of edge cracking are not fully consistent with the studying data of the AMZ layers. For example, in the case of the sample of ceramic laminate Lam SymA in the AMZ layers with a layer thickness 0,029 mm and 0,022 mm no edge cracks were predicted, but in fact after watching these layers by microscope edge cracks were found. On the other hand, in the case of specimens Lam V3A and Lam V5B the predicted existence of edge cracks by the modelling and the existence of edge cracking in prepared samples are completely coincide.

Further, results of the studying the samples prepared by EPD are shown in the Table 4.4. According to the data from the table below it is seen that the predicted the presence and absence of edge cracking by investigation [40] coincide with the presence and absence of edge cracking in the samples prepared by EPD, except sample Lam V3/9. The AMZ layer with layer thickness 0.057 mm of Lam V3/9 has edge cracks, but no edge cracking was predicted for this layer thickness.

Table 4.3. The presence of edge cracking in the AMZ layers prepared by slip casting.

Ceramic laminate	Layer thickness t(AMZ) [mm]	Residual stress in compressive AMZ layer [MPa]	The presence of edge cracks by model [40]	The presence of edge cracks in prepared laminates
Lam SymA	0.029	-719	**no**	**yes**
	0.022		**no**	**yes**
	0.076		yes	yes
	0.069		yes	yes
Lam V3A	0.181	-652	yes	yes
	0.050		yes	yes
	0.019		no	no
	0.107		yes	yes
Lam V5A	0.167	-650	yes	yes
	0.038		**no**	**yes**
	0.039		no	no
	0.141		yes	yes
Lam SymB	0.2868	-454	**yes**	**no**
	0.2208		yes	yes
	0.3176		**yes**	**no**
Lam V3B	0.303	-472	yes	yes
	0.0819		**no**	**yes**
	0.2773		yes	yes
Lam V5B	0.2909	-428	yes	yes
	0.092		no	no
	0.5855		yes	yes

Table 4.4. The presence of edge cracking in the AMZ layers prepared by EPD.

	Layer thickness t(AMZ) [mm]	Residual stress in compressive AMZ layer [MPa]	The presence of edge cracks by model [40]	The presence of edge cracks in prepared laminates
Lam V3/9	0.262	-431	yes	yes
	0.054		no	no
	0.057		**no**	**yes**
	0.309		yes	yes
Lam V5/7	0.268	-403	yes	yes
	0.056		no	no
	0.2898		yes	yes
Lam V3/7	0.265	-433	yes	yes
	0.111		no	no
	0.302		yes	yes
Lam SymP2/9	0.198	-424	yes	yes
	0.392		yes	yes
	0.577		yes	yes
	0.746		yes	yes

By using the model that is described above [40] the value of residual stresses σ_{res}(AMZ) in compressive layer, which are calculated in previous chapter, and their layer thickness t(AMZ)

measured by confocal microscope were estimated. Compositions σ_{res}(AMZ)and t(AMZ) were applied to the graph (see Fig. 4.8) below to visualize.

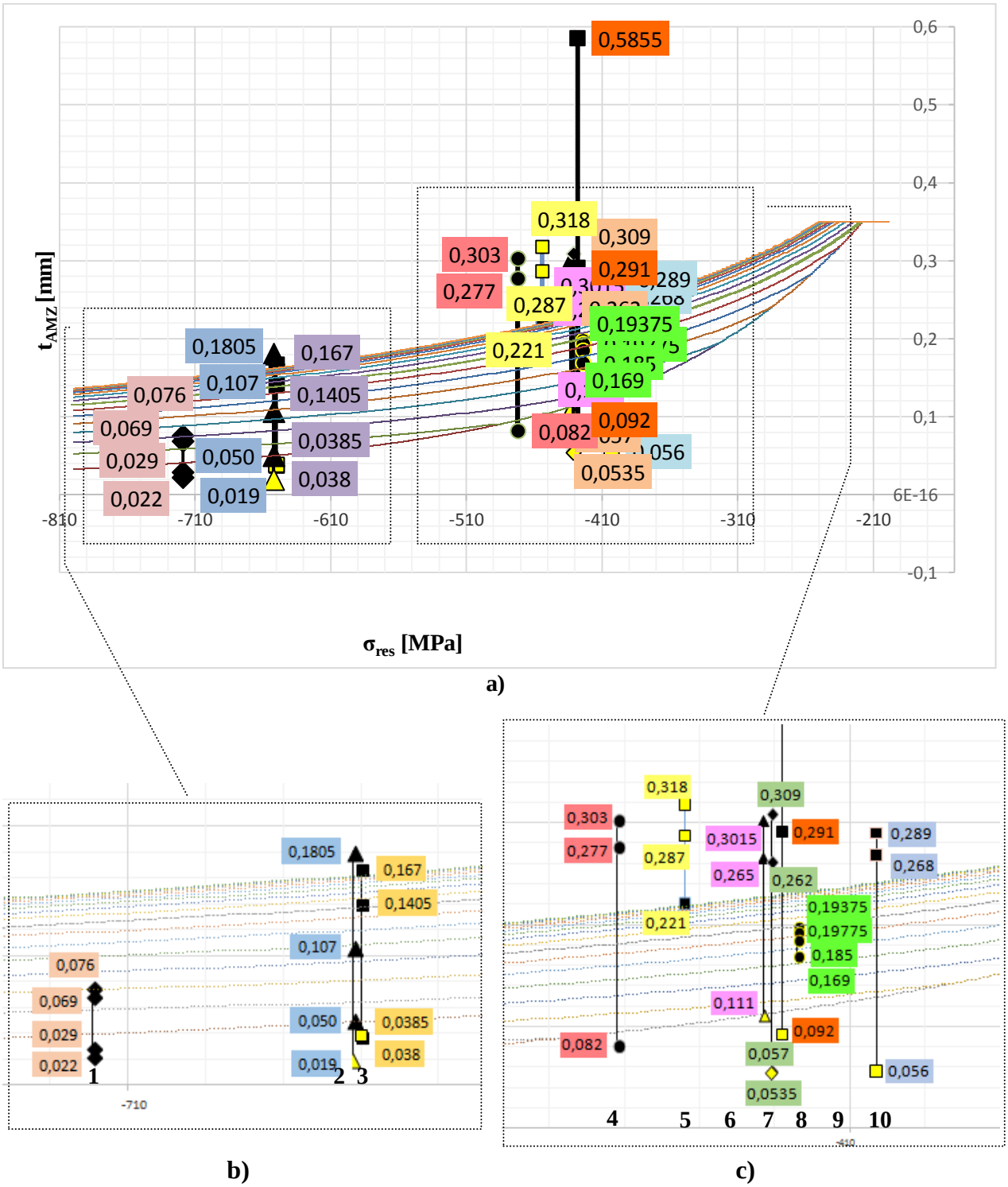

Fig. 4.8. Curves of compositions σ_{res}(AMZ)and t(AMZ) obtained in work [40]; single points of compositions σ_{res}(AMZ)and t(AMZ) connected by a trend line which are obtained in this investigation (a); (b) and (c) are enlarged parts of the graph, where: 1 - Lam SymA, 2 - Lam V3A, 3 - Lam V5A, 4 – Lam V3B, 5 – Lam SymB, 6 – Lam V3/7, 7 – Lam V3/9, 8 – Lam V5B, 9 – Lam SymP2/9, 10 – Lam V5/7.

This graph shows curves obtained during the investigation [40]. The curves exhibit how the residual stresses varies depending on the thickness of the compression AMZ layer. Single

points on the graph connected by a trend line mean composition of residual stress $\sigma_{res}(\mathrm{AMZ})$ and layer thickness $t(\mathrm{AMZ})$ that were obtained in this work in chapters 4.2 and 4.1, respectively. As it is seen, some points of such values are painted in black colour, which means that edge cracks are appearing in the compressive AMZ layers at certain values of residual stress and layer thickness. In the contrary, in the case of single points painted in yellow colour, means that no edge cracking was found in such compositions $\sigma_{res}(\mathrm{AMZ})$and $t(\mathrm{AMZ})$ in prepared samples of ceramic laminates.

Based on the above mentioned it can be concluded that the obtained compositions of calculated and measured residual stresses and AMZ layer thickness, respectively, by using the applied model [40], the prediction of edge crack formation and propagation of prepared samples of 7-layered and 9-layered ceramic laminates by EPD and slip casting in fact is not fully coincides. The reasons of this can be different material properties of prepared samples and the samples applied for the modelling in the [40]. Material properties may be different due to the porosity of the materials or because of small amount undissolved agglomerates of raw powder.

4.4 Analysis of fracture surfaces

The fracture surfaces of the tested specimens were recorded in 3D by using laser confocal microscope at the overview zoom 5×. In this chapter attention will be paid to the differences in fracture behaviour of specimens intended for test of flexural strength. Fig. 4.9, Fig. 4.10 and Fig. 4.11 show fracture surface of samples produced from bi-component materials ATZ and AMZ.

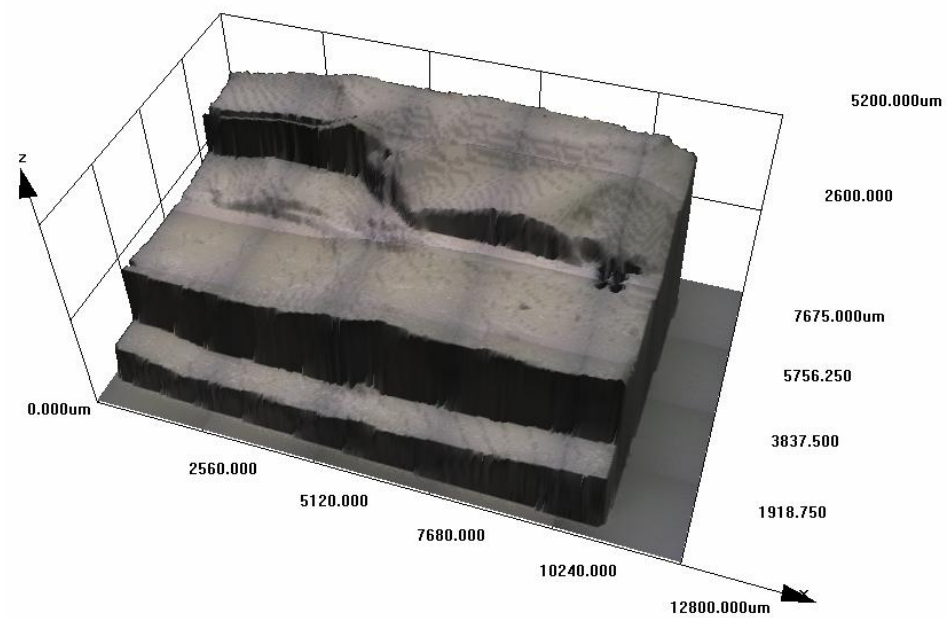

Fig. 4.9. Preview of fracture surface of 9-layered Lam Sym prepared by slip casting.

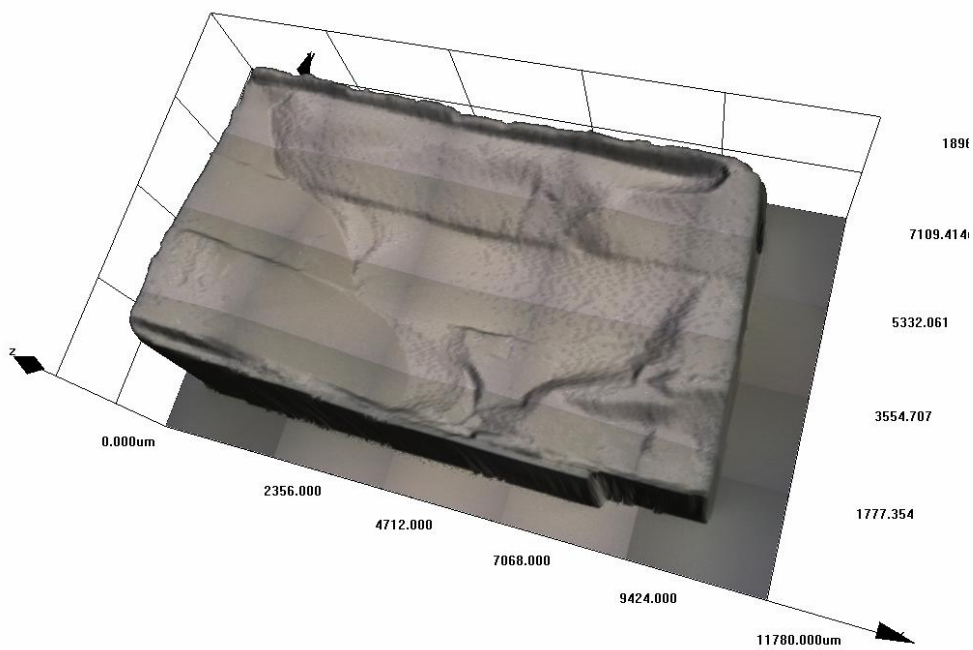

Fig. 4.10. Preview of fracture surface of 9-layered Lam V3A prepared by slip casting.

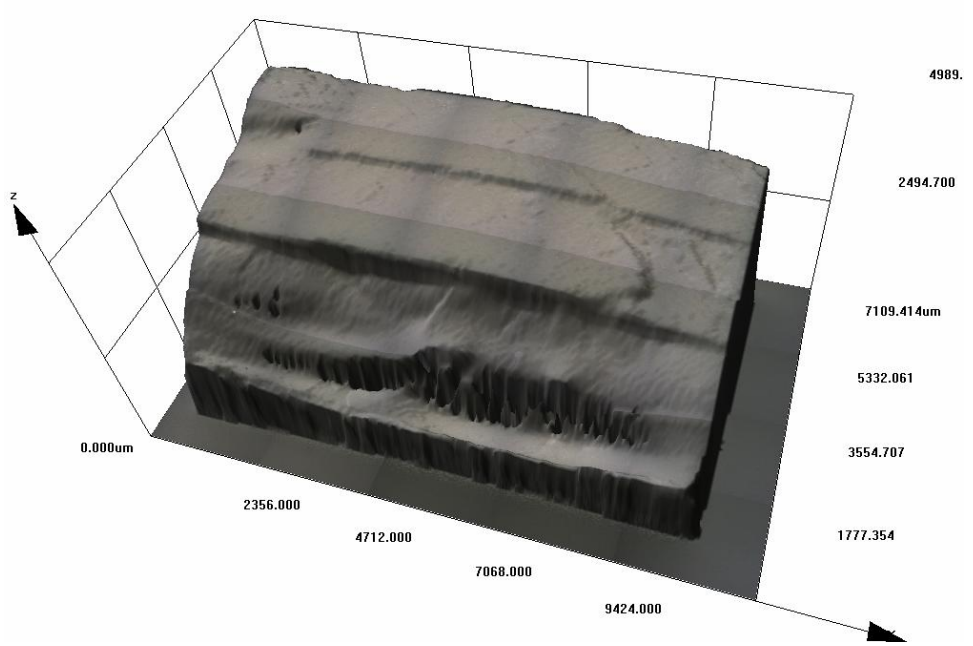

Fig. 4.11. Preview of fracture surface of 9-layered Lam V5A prepared by slip casting.

From fracture surfaces of specimens for determining the flexural strength of multilayer ceramics it is apparent that the deflection of the cracks is partially occurred. Individual steps created by crack diversion are visible on fracture surfaces.

Fig. 4.12, Fig. 4.13 and Fig. 4.14 show fracture surfaces of 7-layered ceramic laminates. The fracture of Lam V5B occurred as well as the fracture of 9-layered ceramic laminates. From Fig. 4.13 and Fig. 4.14 it is seen that the crack propagation was complicated, its body did not extend in-plane of layers and it is difficult to observe the influence of internal compressive and tensile stresses.

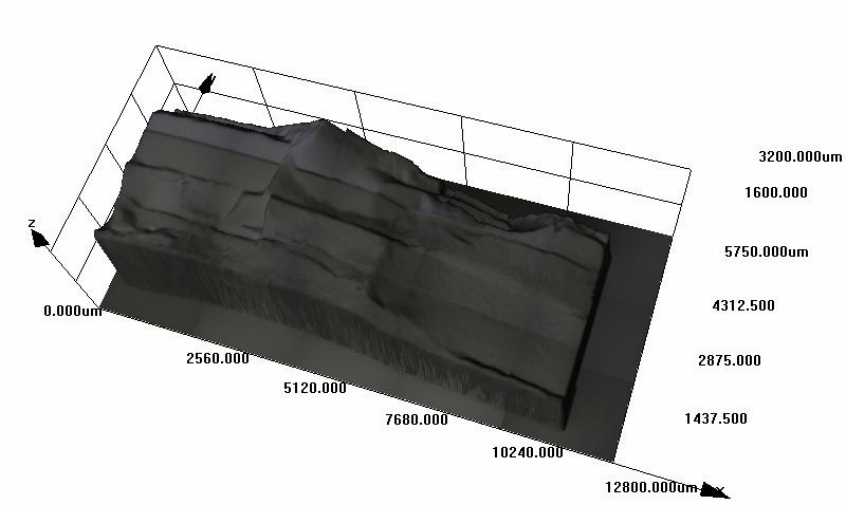

Fig. 4.12. Preview of fracture surface of 7-layered Lam V5B prepared by slip casting.

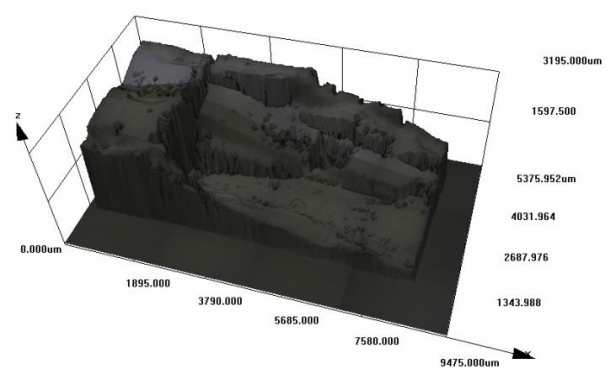

Fig. 4.13. Preview of fracture surface of 7-layered Lam V3B prepared by slip casting.

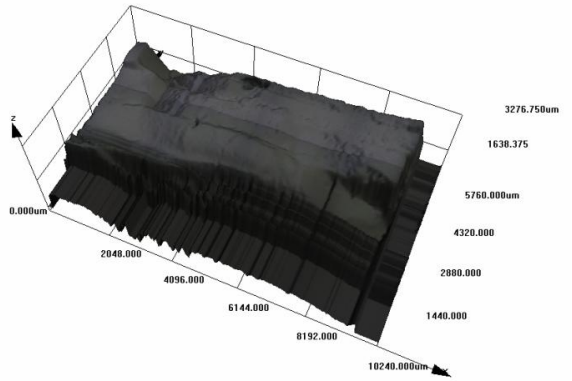

Fig. 4.14. Preview of fracture surface of 7-layered Lam Sym prepared by slip casting.

The fracture surfaces of the ceramic laminates prepared by EPD are shown below in Fig. 4.15 - Fig. 4.18.

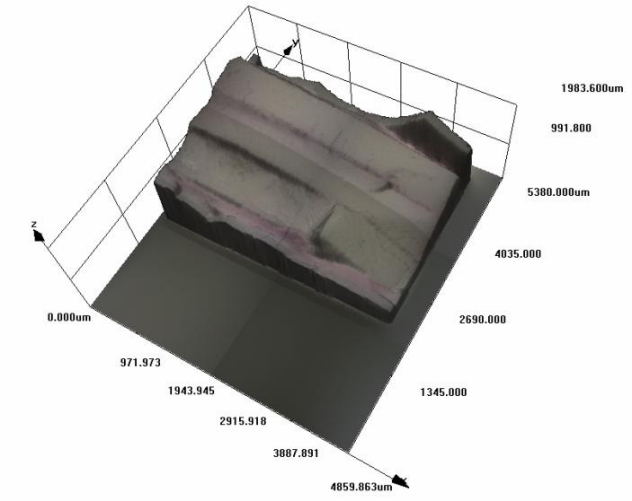

Fig. 4.15. Preview of fracture surface of 9-layered Lam V3/9 prepared by EPD.

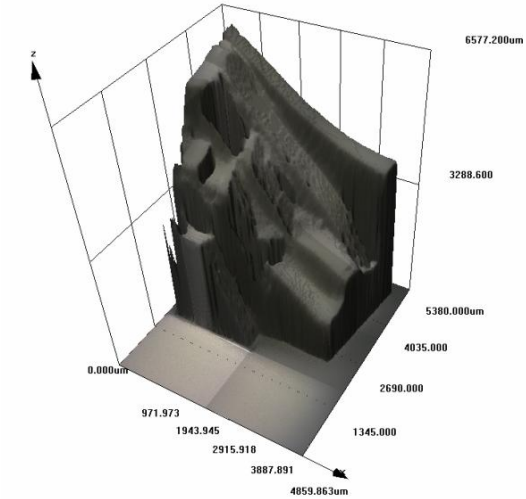

Fig. 4.16. Preview of fracture surface of 9-layered Lam SymP2/9 prepared by EPD.

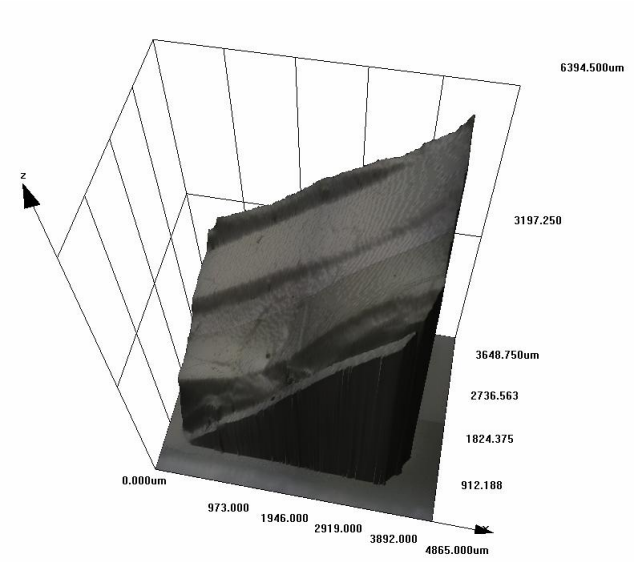

Fig. 4.17. Preview of fracture surface of 7-layered Lam V3/7 prepared by EPD.

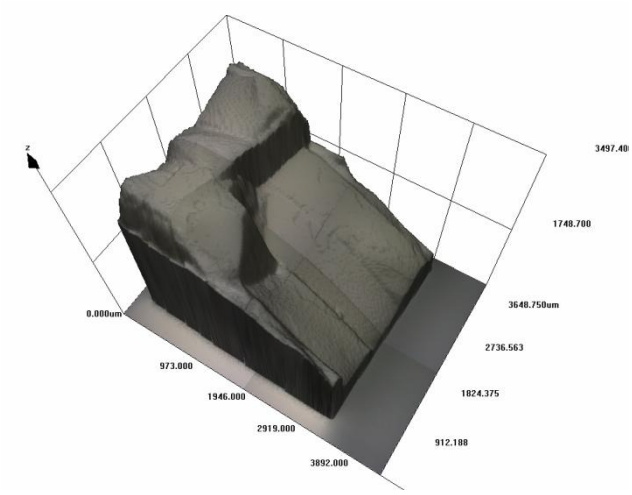

Fig. 4.18. Preview of fracture surface of 7-layered Lam V5/7 prepared by EPD.

By presented figures above it is clearly seen that crack propagations during the fracture were complicated, not in-plane the layers. For example, from fracture surface of sample Lam SymP2/9 (see Fig. 4.16) it is clear that the crack propagation repeatedly changed the direction. Crack propagated from ATZ layer toward the AMZ layer perpendicularly to the interface between two layers, while crack propagated from AMZ layer to ATZ layer with the change of direction towards the interface. Such phenomenon is termed as crack bifurcation. 3D pictures also show that the largest deviation of the crack occurs inside the samples than at the surfaces. The reason of such behaviour may be the presence of residual stresses, which are also the cause of edge cracking. Based on this it can be assumed that the edge cracking has an effect on the crack bifurcation.

4.5 Flexural strength

All 9 samples of ceramic laminates were tested for flexural strength. It should be noted that the ceramic laminates consisted of 7 alternated layers of two different materials were obtained with poor quality. Initially they were cracked and hence it can be assumed that such cracking has an impact during the testing of samples on flexural strength. Also mechanical properties of these laminates were obtained as poor values because probably the cracking occurred already during the cooling from sintering temperature. Further in the following paragraphs there are graphs which show the load increases over time depending on the sample, and the corresponding to the curves the fracture surfaces.

4.5.1 Ceramic laminates prepared by slip casting

From the fracture surface that are shown in figures Fig. 4.19 - Fig. 4.24 it is visible how curves of loading correspond to them. For example on the graph in Fig. 4.20 a smooth increase of loading over time is clearly seen and the same is markedly on fracture surface. The fracture surface does not have a sharp transitions and steps.

On the contrary to the above, Fig. 4.24 shows a loading curve of sample Lam V5B and it can be seen that the loading was uneven and the fracture surface has a characteristic relief. The changes of the trajectory of crack propagation at the interface run gradually and it is noticeable that it is affected by the internal residual stresses.

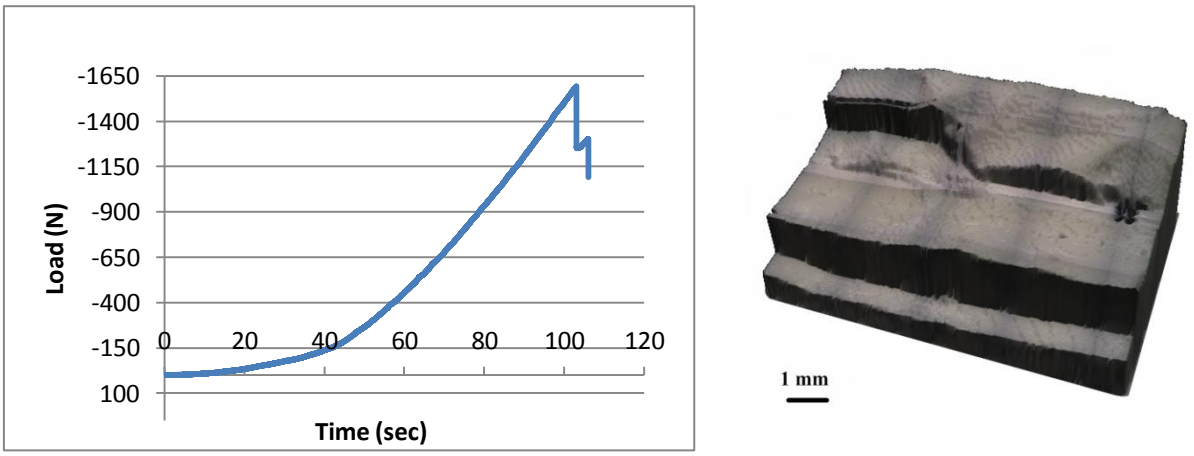

Fig. 4.19. Loading of the sample Lam SymA depending on the time and its fracture surface

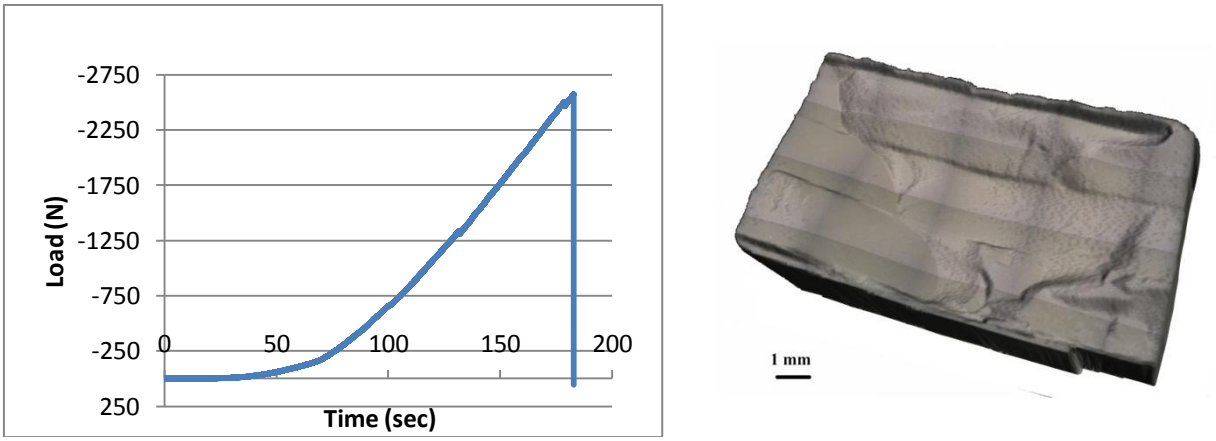

Fig. 4.20. Loading of the sample Lam V3A depending on the time and its fracture surface

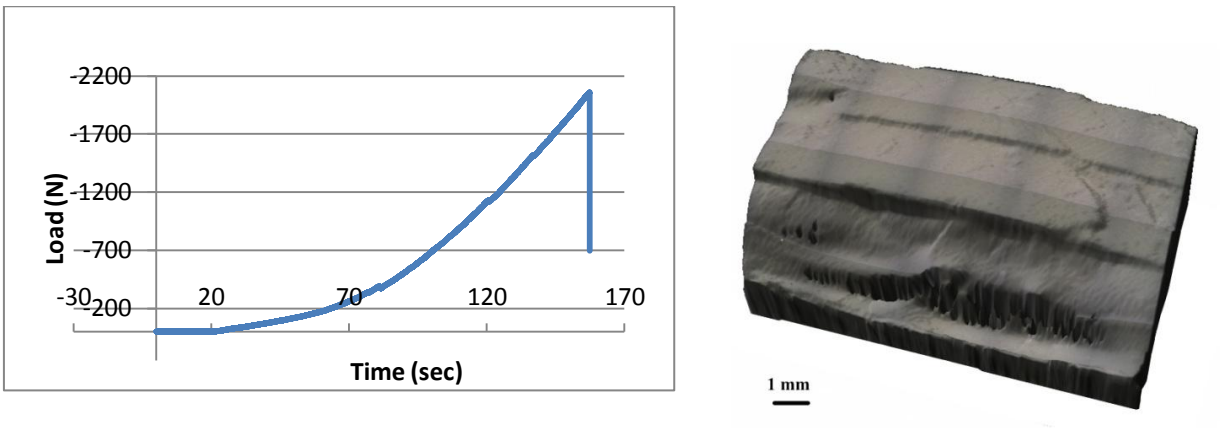

Fig. 4.21. Loading of the sample Lam V5A depending on the time and its fracture surface

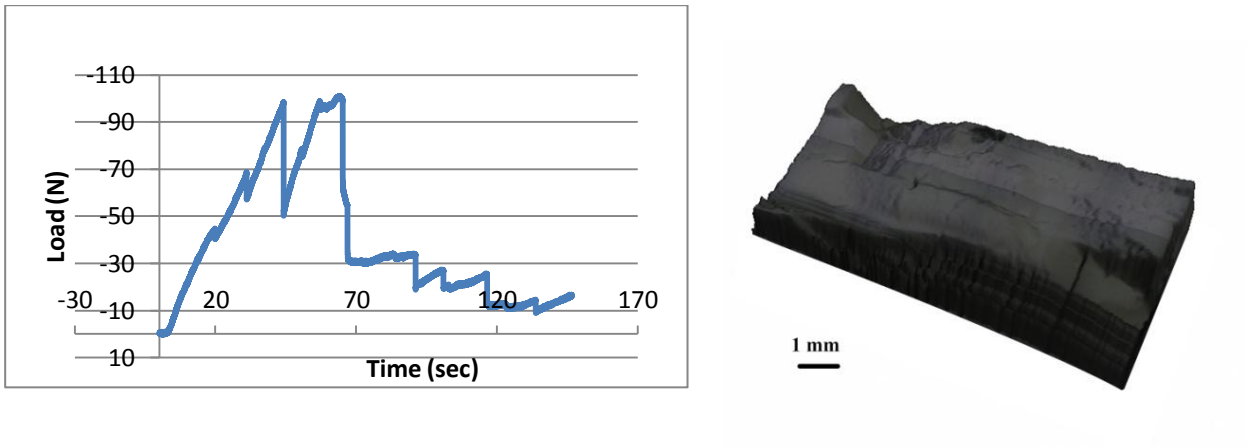

Fig. 4.22. Loading of the sample Lam SymB depending on the time and its fracture surface

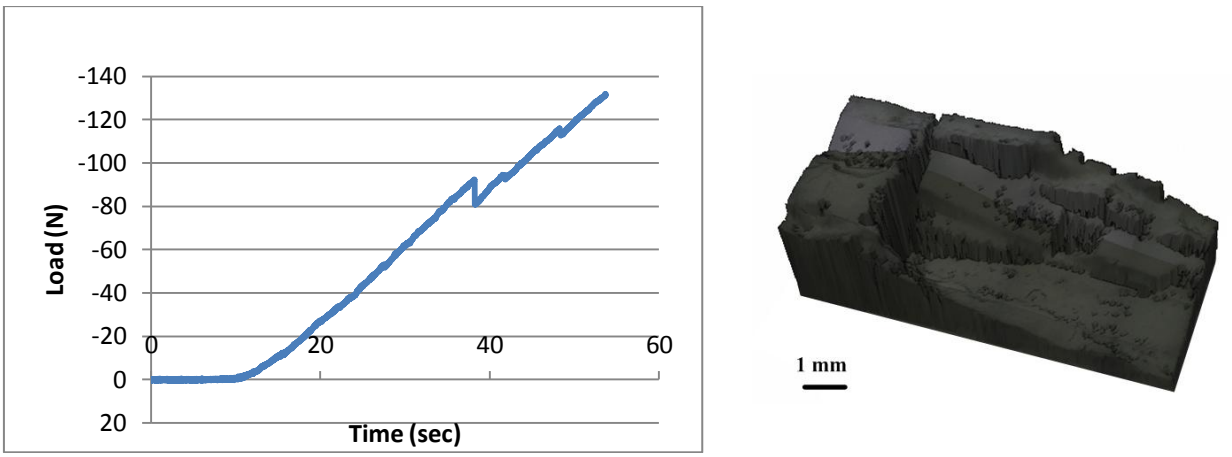

Fig. 4.23. Loading of the sample Lam V3B depending on the time and its fracture surface

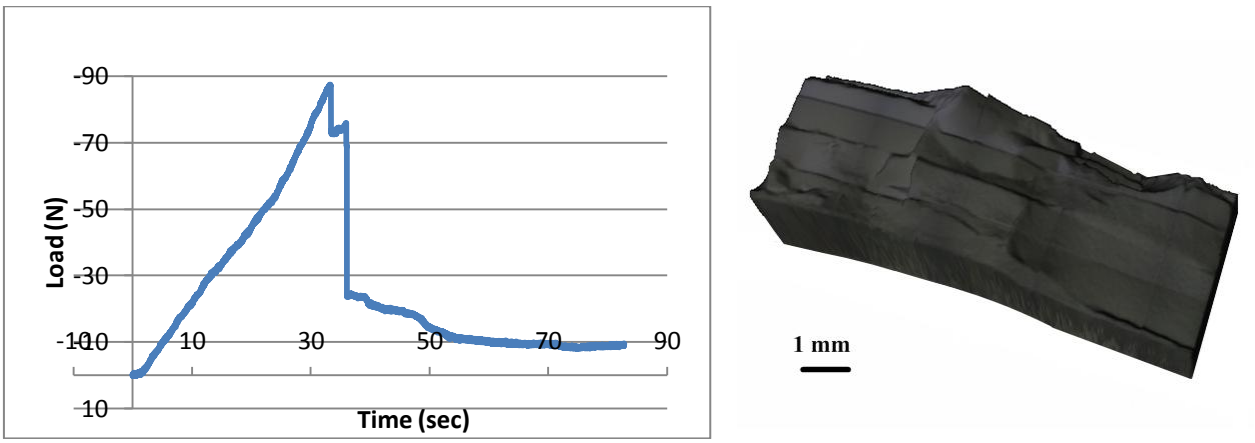

Fig. 4.24. Loading of the sample Lam V5B depending on the time and its fracture surface

Data of flexural strength test are shown in Table 4.5. From this table it is clearly evident that the biggest loading for the break of sample was applied to Lam V3A consisting of 9 alternating layers, and the lowest load was applied to the sample Lam V5B, which consists of 7 alternating layers. Hence, the Lam V3A has a highest flexural strength, as it can see from Fig. 4.25, σ_f=452,75 MPa that was calculated by equation (4.4) [15]:

$$\sigma_f = \frac{3 * F_m * l}{2 * b * h^2} \tag{4.4}$$

where F_m is maximum load, b is the beam height, h is thickness and l is distance between the supporting pins.

Table 4.5: Test results ceramic laminates prepared by slip casting.

Material	Width [mm]	Thickness [mm]	Load [N]	Flexural strength σ_f [MPa]
Lam SymA	>10,040	>6,040	1592,10	260,80
Lam V3A	>10,030	>5,830	2572,37	452,74
Lam V5A	>10,040	>5,910	2059,83	352,43
Lam SymB	>8,500	>4,100	101,06	42,44
Lam V3B	>8,310	>3,810	131,81	65,56
Lam V5B	>10,230	>4,040	87,48	31,44

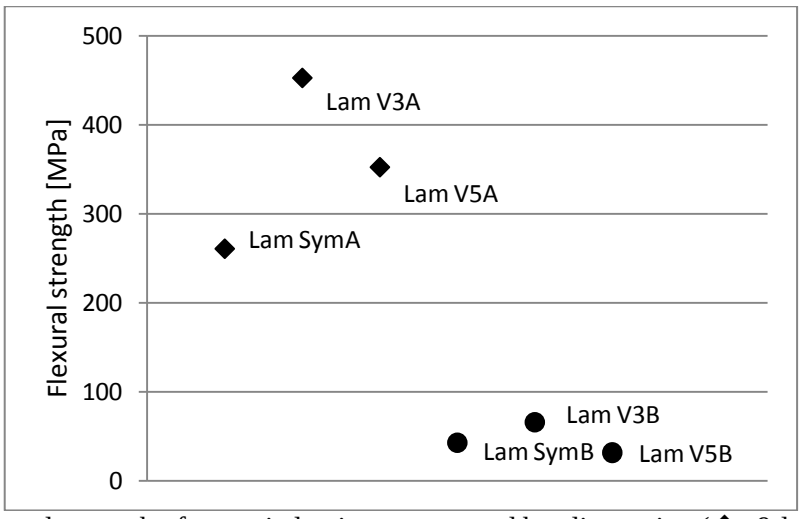

Fig. 4.25. Flexural strength of ceramic laminates prepared by slip casting (◆- 9-layered ceramic laminates, ●- 7 layered ceramic laminates)

4.5.2 Ceramic laminates prepared by EPD

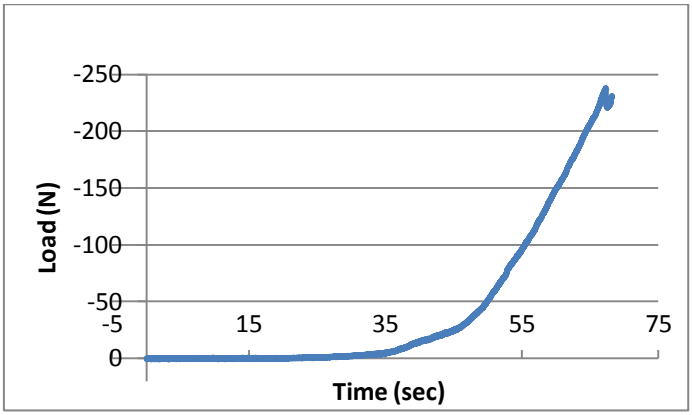

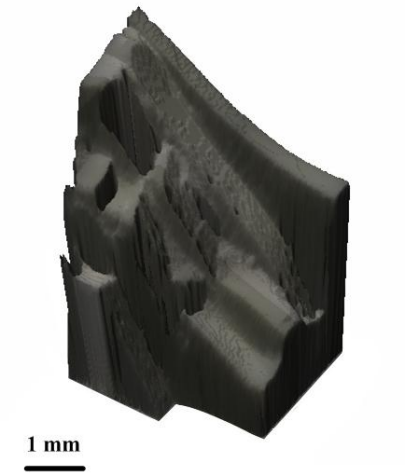

Fig. 4.26. Loading of the sample Lam SymP2/9 depending on the time and its fracture surface.

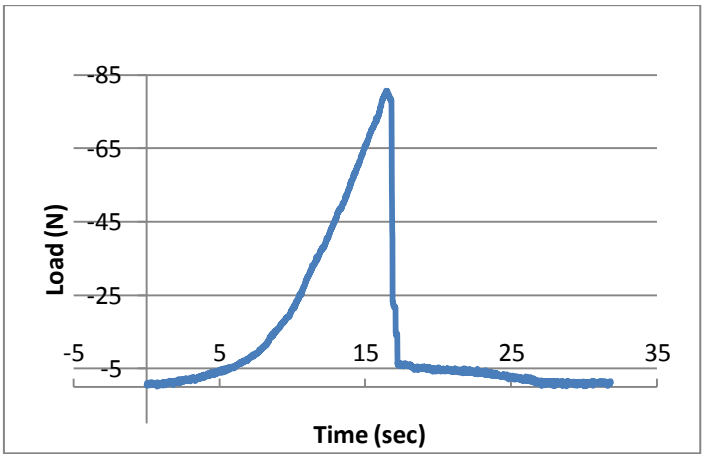

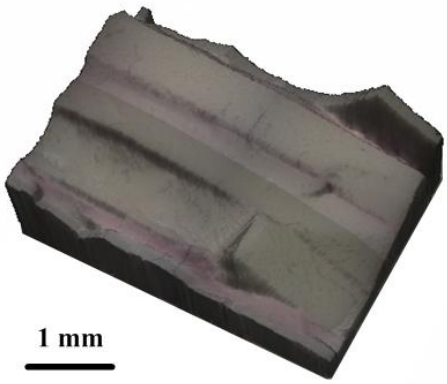

Fig. 4.27. Loading of the sample Lam V3/9 depending on the time and its fracture surface.

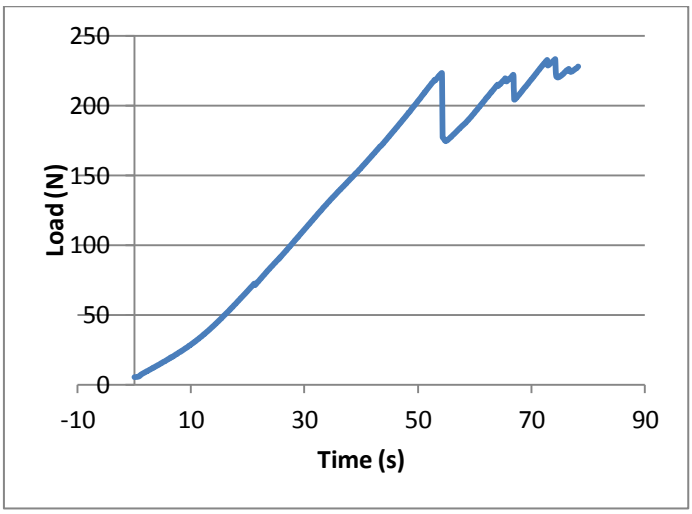

Fig. 4.28. Loading of the sample Lam V3/7 depending on the time and its fracture surface.

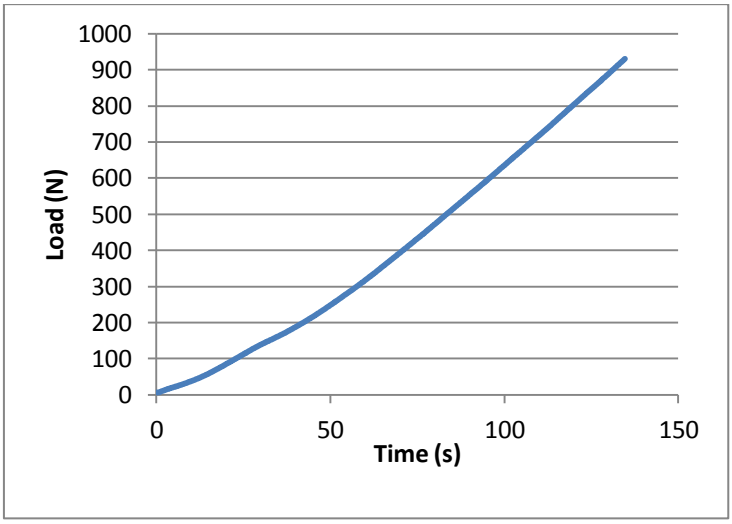

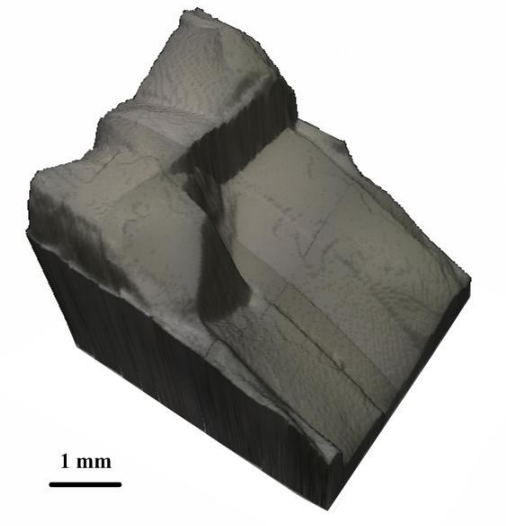

Fig. 4.29. Loading of the sample Lam V5/7 depending on the time and its fracture surface.

From the loading curve (see Fig. 4.26), which belongs to the sample Lam Sym/9, it is seen that the fracture occurs uniformly without sharp drops, which is the same as sample Lam V5/7 (see Fig. 4.29), while on the surface of fracture the obvious steps are seen, which means that the crack propagation changes the direction during crossing the interface of the two layers.

Fig. 4.27 shows the loading curve of ceramic laminate Lam V3/9. After reaching the maximum value of the applied force, there was a sharp drop down quickly after the test beginning. This means that the laminate has a small value of flexural strength.

On the contrary, the loading curve of sample Lam V3/7 shows the loading was uneven and the fracture surface has a characteristic relief. The changes of the trajectory of crack propagation at the interface run gradually and it is noticeable that it is affected by the internal residual stresses. Table 4.6 shows the results of testing on flexural strength and calculated values of strength by the equation (4.4).

Table 4.6: Test results of ceramic laminates prepared by EPD.

Material	Width [mm]	Thickness [mm]	Load [N]	Flexural strength σ_f [MPa]
Lam SymP2/9	>4,250	>3,280	238,33	125,10
Lam V3/9	>4,330	>3,080	80,76	47,19
Lam V3/7	>4,09	>2,94	228,02	193,5
Lam V5/7	>4,38	>3,14	931,57	647,15

Fig. 4.30 shows that the Lam V5/7 has a highest flexural strength, $\sigma_f = 647{,}15$ [MPa], while the Lam V3/9 has the lowest value of flexural strength.

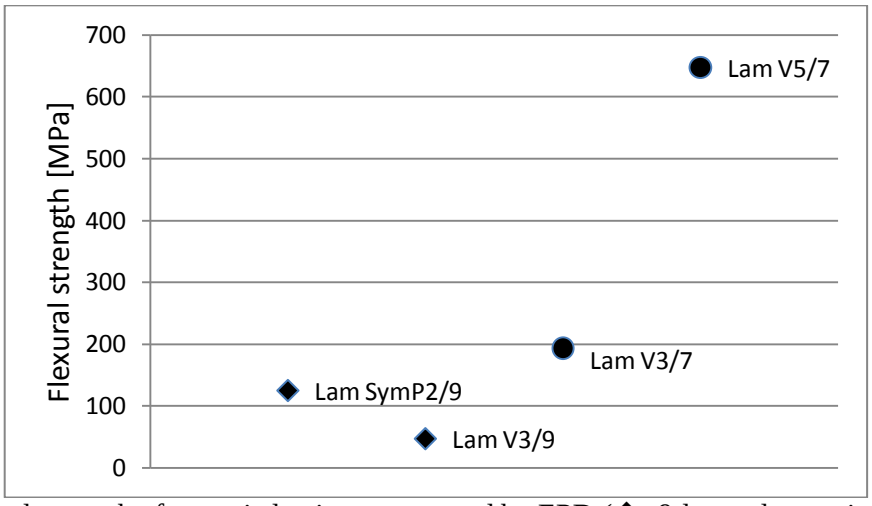

Fig. 4.30. Flexural strength of ceramic laminates prepared by EPD (◆- 9-layered ceramic laminates, ●- 7 layered ceramic laminates).

5 CONCLUSIONS

The ceramic laminates combining, at least, layers of two different ceramic materials are promising way to make fracture resistant advanced ceramic. The several approaches for ceramic layers preparation were developed during last decades based on introduction of weak or strong interfaces between layers to attain crack stopping and/or crack divergence. The most promising way is to introduce the residual internal stresses serves as a crack closing force.

The overall value of the residual stresses in the laminate depends on the volume ratio of materials combined. By changing the thickness of individual layers in the composite the residual stresses can be directly redistributed over the laminate. Depending on the value of residual stresses in the layer the growing crack will be either stopped or deflected. The tensile residual stresses can serve as very efficient way how to deflet growing crack along layer interface. The strongly bonded laminates than thus utilize the same mechanism as in the case of weakly bonded laminates but they are maintaining their excellent strength characteristics.

In this work, six samples and four samples of 7 and 9 layered ceramic laminates consisted of AMZ (60,5% α-Al_2O_3 + 39,5% monoclinic-ZrO_2) and ATZ (92,6% α-Al_2O_3 + 7,4% tetragonal-ZrO_2)layers were prepared by sequential slip casting and electrophoretic deposition, respectively.

The homogeneity, structure and mechanical properties of the laminate prepared were studied. It was observed that the samples have a porosity and delamination between layers in some places as a consequence of porosity.

The value of the residual stresses in compressive layers of the laminates was calculated. The 9 layered sample Lam Sym A (symmetrical laminate containing XX% of ATZ and XX% of AMZ), which has a symmetric architecture, has the highest value of residual stresses, $\sigma_{res} = 719\ MPa$. Based on a literature review from the first chapter it can be concluded that such high values of residual stresses may contribute to the formation of edge cracks at the free surface. Cracks propagate deep into the sample in-plane the AMZ layer. Each prepared sample has an edge cracking depending on the thickness of individual layers and thus on the value of residual stresses.

Further, applying the results of 2D parametric numerical model the prediction of presence and absence of edge cracking were compared with actual presence or absence of edge cracks in compressive layers. Based on the results of this comparison, it can be concluded that the prediction of formation and propagation of edge cracking in compressive layers of prepared ceramic laminates is not fully coincides. The reason of this can be different material properties of

prepared samples and the samples applied for the 2D model. Also the difference between properties of those materials may be due to porosity or small amount of undissolved particles of raw powder.

Then the crack bifurcation was studied on the 3D fracture surfaces reconstruction of laminate after testing on flexural strength. The fracture surfaces almost of all samples showed that the crack propagation during the fracture were complicated, not in-plane the layers. There are individual steps created by crack deflection. Crack propagated perpendicularly from ATZ layer to AMZ layer and then it changed direction of propagation towards the interface. Also 3D pictures showed that the largest deviation of the crack occurs inside the samples than at the surface. The reason of such behaviour may be the presence of residual stresses. Hence, it can be assumed that the edge cracking has an effect on the crack bifurcation, because the edge cracking caused by internal residual stresses.

In this work the crack propagation was studied after testing on flexural strength, also the effect on it from the presence of edge cracking, which is formed due to high values of residual stresses. During the testing on flexural strength it was observed that the 7 layered ceramic laminates were obtained with poor quality and poor values of flexural strength. By using the obtained values of the maximum load the flexural strength of all samples were calculated. The sample Lam V3A has a maximum value, while the sample Lam SymA has the lowest value of flexural strength, though it has the maximum value of residual stresses.

6 REFERENCES

[1] KINGERY, W. D., BOWEN, K.H., UHLMAN, R.H. *Introduction to Ceramics.* John Willey & Sons. Inc. 1976. 1032 s. ISBN 0-471-47860-1.

[2] DRDLIK, Daniel. *Vrstevnate keramicke kompozitni materialy – příprava, struktura a vlastnosti*. Brno, 2009. 45 s. Diplomova prace. Vysoke učeni technicke v Brně, Fakulta strojniho inženyrstvi

[3] JIANXIN D, DONGLING Y, HUOMIN Z, YUANQIANG T. Layered structures in ceramic nozzles for improved erosion wear resistance in industrial coalwater-slurry boilers. *Ceram Int* 2010;36(1):299–306.

[4] DUBUS B, HAW G, GRANGER C, LEDEZ O. Characterization of multilayered piezoelectric ceramics for high power transducers. *Ultrasonics* 2002;40(1-8):903–6, 1st Ultrasonics International Conference, Delft, Netherlands, July 03–05, 2001.

[5] JIANXIN D, ZHENXING D, DONGLING Y, HUI Z, XING A, JUN Z. Fabrication and performance of al(2)o(3)/(w,ti)c +al(2)o(3)/tic multilayered ceramic cutting tools. *Mater Sci Eng*, A 2010;527(4–5):1039–47.

[6] CHLUP Z, SALAMON D. Properties of porous multi-layered free-standing ceramic microchannels. *Scr Mater* 2010;63(6):597–600.

[7] ŠESTÁKOVÁ L., *Hodnocení stability obecných koncentrátorů napětí ve vrstevnatých materiálech.* VUT Brno. Fakulta strojního inženýrství, 2009. 33 s. ISBN 978-80-214-3992-4

[8] CLEGG, W. J., et al. A simple way to make tough ceramics. *Nature*. 1990, 347, s. 455-457

[9] PRAKASH, O., SARKAR, P., NICHOLSON, P., Crack Deflection in Ceramic/Ceramic Laminates with Strong Interfaces. *J. Am. Ceram. Soc.*, 1995, roč. 78, č. 4, s. 1125-1127.

[10] RICHERSON, David W. *Modern Ceramic Engineering: Properties, Processing and Use in Design*. 2nd ed. New York: Marcel Dekker, Inc., 1992. 860 s. ISBN 0-8247-8634-3.

[11] MICELE, Lorenzo. *Preparation and characterization of laminated ceramic composites*. Bologna, 2005. 153 s. Dissertation work. University of Bologna, Faculty of Industrial Chemistry, Department of Industrial and Materials Chemistry

[12] HANSEN, J., CUTLER, R., SHETTY, D., VIRKAR, V. Indentation Fracture Response and Damage Resistance of Al_2O_3-ZrO_2 Composites Strengthened by Transformation-Induced Residual Stresses. *J. Am. Ceram. Soc.*, 1988, 71 (12), p. 501-505.

[13] MARSHALL D. B. et al. *Partially stabilized ZrO2 - based laminar ceramic composites*. US 5284698. 1994-02-08.

[14] MARSHALL, B., KATTO, J. Enhanced Fracture Toughness in Layered Microcomposites of Ce-ZrO_2 and Al_2O_3. *J. Am. Ceram. Soc.*, 1991, 74, p. 2979-87.

[15] BERMEJO MORATINOS, Raul *Structural integrity of alumina – zirconia multilayred* ceramics. Barcelona, 2006. XXVIII, 199 s. Dissertation work. Universidad Politecnica de Cataluna.

[16] PRNKA, Tasilo; ŠPERLINK, Karel. *Bionanotechnologie, nanobiotechnologie, nanomedicina*. Ostrava : Repronis, 2006. 177 s.

[17] LUBE, Tanja. Mechanical Properties of Ceramic Laminates. *Key Engineering Materials*. 2007, 337, s. 87-96.

[18] YU, Z. B.; KRSTIC, V. D. Fabrication and characterization of laminated SiC ceramics with self-sealed ring structure. *Journal of materials science*. 2003, 38, s. 4735-4738.

[19] KLIMEŠ, Jan. *Studium šíření trhlin ve vrstevnatém materiálu*. Brno, 2004. 45 p. Master's thesis. Brno University of Technology, Faculty of Mechanical Engineering.

[20] VAN DER BIEST, O., et al. Laminated and functionally graded ceramics by electrophoretic deposition. *Key Engineering Materials*. 2007, vol. 333, s. 49-58.

[21] HATTON, Benjamin; NICHOLSON, Patrick S. Design and Fracture of Layered Al2O3/TZ3Y Composites Produced by Electrophoretic Deposition. *Journal of the American Ceramic Society*. 2001, 84, 3, s. 571-576.

[22] CHLUP, Zdeněk; HADRABA, Hynek. Alumina and Zirconia Based Composites: Part 2 Fracture Response. *Key Engineering Materials*. 2009, 412, s. 227-232.

[23] YUNFEI Chang, Raul BERMEJO, Oldrich SEVECEK, GARY L. Messing Design of alumina-zirconia composites with spatially tailored strength and toughness. *Journal of the European Ceramic Society* 35 (2015) 631-640.

[24] R. BERMEJO, C. Baudín, R. MORENO, L. Llanes, A.J. SANCHEZ-HERENCIA. Processing optimisation and fracture behaviour of layered ceramic composites with highly compressive layers. *Composites Science and Technology*. Volume 67, Issue 9, July 2007, Pages 1930–1938

[25] SANCHEZ-HERENCIA, A.J., PASCUAL, C., He, J., LANGE, F.F. ZrO2/ZrO2 layered composites for crack bifurcation. *Journal of the American Ceramic Society*. Volume 82, Issue 6, 1999, Pages 1512-1518

[26] TANDON, R. and GREEN, D.J. "Crack Stability and T-Curves due to Macroscopic Residual Compressive Stress Profiles", *J. Am. Ceram. Soc.*, 74, 1981-6 (1991)

[27] CUTLER, R.A., BRIGHT, J.D., VIRKAR, A.V. and SHETTY, D.K. "Strength Improvement in Transformation-Toughened Alumina by Selective Phase- Transformation", *J. Am. Ceram. Soc.*, 70, 714-8 (1987)

[28] RAO, M.P., SANCHEZ-HERENCIA, A.J., BELTZ, G.E., McMEEKING, R.M. and LANGE, F.F. "Laminar Ceramics that Exhibit a Threshold Strength", *Science*, 286, 102-5 (1999)

[29] ZUO, Kai Hui; JIANG, Dong Liang; LIN, Qing Ling. Fabrication and interfacial structure of Al_2O_3/Ni laminar ceramics. *Ceramics International*. 2006, 32, 6, s. 613-616.

[30] *Britannica Online Encyclopedia* [online]. 2010 [cit. 2010-03-21]. Doctor blading. Available from WWW: <http://www.britannica.com/EBchecked/topic-art/583086/262/Steps-indoctor-blading-a-tape-casting-process-employed-in>.

[31] PORTU, G. de; MICELE, L.; PEZZOTTI, G. Laminated ceramic structures from oxide systems. *Composites: Part B: engineering*. 2006, 37, s. 556-567

[32] LUCCHINI, E.; SBAIZERO, O. Alumina/Zirconia Multilayer Composites Obtained by Centrifugal Consolidation. *Journal of the European Ceramic Society*. 1995, 15, s. 975-981.

[33] HADRABA, Hynek; MACA, Karel; CHLUP, Zdeněk. Alumina and Zirconia Based Composites: Part 1 Preparation. *Key Engineering Materials*. 2009, vol. 412, s. 221-226.

[34] HADRABA, H.; MACA, K.; CIHLAŘ, J.. Electrophoretic deposition of alumina and zirconia - II. Two-component systems. *Ceramics International*. 2004, 30, s. 853-563.

[35] SARKAR, P.; DATTA, S.; NICHOLSON, P.S. Functionally graded ceramic/ceramic and metal/ceramic composites by electrophoretic deposition. *Composites. Part B, Engineering*. 1997, 28, 1-2, s. 49-56.

[36] HADRABA, H. Doctoral thesis - Functional gradient ceramic materials. VUT Brno, 2002.

[37] EN 843-1. Advanced technical ceramics. Mechanical properties of monolithic ceramics at room temperature. Determination of flexural strength; 2007.

[38] *Index of http://www.isfk.at* [online]. 2012 [2012-01-15] Laminate Theory (web-App). Available from WWW: <http://wm.unileoben.ac.at:8080/webMathematica/ISFK/Laminate_Theory_webApp.jsp>

[39] *Index of http://www.isfk.at* [online]. 2012 [2012-01-15] Classical Laminate Theory (CLT). Available from WWW: http://www.isfk.at/de/1428/

[40] SEVECEK, O., KOTOUL, M., LEGUILLON, D., MARTIN, E., BERMEJO, R. Modelling of edge crack formation and propagation in ceramic laminates using the stress – energy coupled criterion. *Engineering Fracture Mechanics*. 2016.

[41] S. HO, C. HILLMAN, F.F. LANGE, Z. SUO. Surface cracking in layers under biaxial, residual compressive stress. *J Am Ceram Soc*, 78 (1995), pp. 2353–2359

7 NOMENCLATURE

Magnitudes

α	[K^{-1}]	coefficient of linear thermal expansion
$\Delta\alpha$	[-]	direction of crack propagation
b	[m]	height
d	[m]	distance of the electrods
e	[m]	wall thickness
E	[MPa]	elastic modulus
E_e	[V*m^{-1}]	electric field intensity
F_m	[N]	load
G	[-]	tensile stress field
G_{inc}	[-]	energy release rate
h	[mm]	thickness of sample
K_{IC}	[MPa*$m^{-1/2}$]	fracture toughness
k	[-]	kinetic constant
l	[mm]	distance between the supporting pins
m_0	[kg]	initial weight of the particles in the suspension
	[m^2*V^{-1}]	electrophoretic mobility
$\sigma_a \sigma_b$	[MPa]	residual stress in composition A and B
$\sigma_{yy,x}$	[MPa]	tensile stress
σ_R	[MPa]	compressive stress
σ_c	[MPa]	critical tensile stress
σ_{yy}	[MPa]	stress along the prospective crack path
σ_f	[MPa]	flexural strength
$\bar{t}$	[µm]	average layer thickness
t_a, t_b	[µm]	layer thickness of compositions A and B
t	[s]	casting time
t_c	[µm]	critical layer thickness
ΔT	[°C]	temperature increment
ν	[-]	Poisson's ratio
W(a)	[-]	potential energy of cracked body
W(0)	[-]	potential energy of uncracked body

Abbreviations

AMZ	Alumina with monoclinic zirconia
ATZ	Alumina with tetragonal zirconia
CC	Coupled criterion
DC	Direction current
EPD	Electrophoretic deposition
ERR	Energy release rate
FE	Finite element
PN	Pierels-Nabarro

8 LIST OF FIGURES

9 LIST OF TABLES